HHS Public Access

Author manuscript

Br J Pharmacol. Author manuscript; available in PMC 2022 October 01.

Published in final edited form as:

Br J Pharmacol. 2021 October ; 178(19): 3905–3923. doi:10.1111/bph.15531.

Inhibition of inflammatory pain and cough by a novel charged sodium channel blocker

Ivan Tochitsky[1,*], **Sooyeon Jo**[2,*], **Nick Andrews**[1], **Masakazu Kotoda**[1], **Benjamin Doyle**[1], **Jaehoon Shim**[1], **Sebastien Talbot**[1,3], **David Roberson**[1], **Jinbo Lee**[4], **Louise Haste**[5], **Stephen M. Jordan**[5], **Bruce D. Levy**[6,#], **Bruce P. Bean**[2,#], **Clifford J. Woolf**[1,2,#]

[1]F.M. Kirby Neurobiology Research Center, Boston Children's Hospital, Boston, MA 02115

[2]Department of Neurobiology, Harvard Medical School, Boston MA 02115

[3]Départément de Pharmacologie et Physiologie, Université de Montréal, Canada

[4]Sage Partner International, Andover MA 01810

[5]Covance Inc., Woolley Rd, Alconbury, Huntingdon PE28 4HS, United Kingdom

[6]Pulmonary and Critical Care Medicine, Department of Internal Medicine, Brigham and Women's Hospital, Harvard Medical School, Boston, MA 02115, USA

Abstract

Background and Purpose: Many pain-triggering nociceptor neurons express TRPV1 or TRPA1, cation-selective channels with large pores that enable permeation of QX-314, a cationic analogue of lidocaine. Co-application of QX-314 with TRPV1 or TRPA1 activators can silence nociceptors. In this study, we describe BW-031, a novel more potent cationic sodium channel inhibitor, test whether its application alone can inhibit pain associated with tissue inflammation, and whether this strategy can also inhibit cough.

Experimental Approach: We tested the ability of BW-031 to inhibit pain in three models of tissue inflammation: inflammation in rat paws produced by Complete Freund's Adjuvant or by surgical incision and a mouse UV burn model. We tested the ability of BW-031 to inhibit cough induced by inhalation of dilute citric acid in guinea pigs.

Correspondence to B.D.L., B.P.B. and C.J.W.

*These authors contributed equally: Ivan Tochitsky, Sooyeon Jo.

#Co-senior authors

Author Contributions

I.T., S.J., N.A., M.K., B.D.L., B.P.B. and C.J.W. designed experiments; I.T., S.J., N.A., M.K., B.D., J.S., S.T., D.R., J.L., L.H., S.M.J. carried out experiments; I.T., S.J., N.A., M.K., B.D., J.S., L.H. and S.M.J. analyzed data; I.T., S.J., N.A., M.K., B.D., J.S., B.D.L., B.P.B. and C.J.W. provided advice on the interpretation of data; I.T., B.D.L, B.P.B and C.J.W. wrote the manuscript with input from all co-authors; B.D.L., B.P.B., and C.J.W. supervised the study. All authors approved the final manuscript.

Conflict of Interest

B.D.L., B.P.B. and C.J.W. are cofounders of and equity holders in Nocion Therapeutics which is developing charged sodium channel blockers as treatments for various disease indications, including cough, and which has licensed BW-031 from Harvard Medical School. I.T., S.J., N.A., S.T. and D.R. also have founder shares in Nocion.

Declaration of Transparency and Scientific Rigour

This Declaration acknowledges that this paper adheres to the principles for transparent reporting and scientific rigour of preclinical research as stated in the BJP guidelines for Design & Analysis and as recommended by funding agencies, publishers and other organisations engaged with supporting research.

Key Results: BW-031 inhibited $Na_v1.7$ and $Na_v1.1$ channels with ~6-fold greater potency than QX-314 when introduced inside cells. BW-031 inhibited inflammatory pain in all three models tested, producing more effective and longer-lasting inhibition of pain than QX-314 in the mouse UV burn model. BW-031 was effective in reducing cough counts by 78-90% when applied intratracheally under isoflurane anesthesia or by aerosol inhalation in guinea pigs with airway inflammation produced by ovalbumin sensitization.

Conclusion and Implications: BW-031 is a novel cationic sodium channel inhibitor that can be applied locally as a single agent to inhibit inflammatory pain. BW-031 can also effectively inhibit cough in a guinea pig model of citric acid induced cough, suggesting a new clinical approach to treating cough.

Introduction

Most clinically-used local anaesthetics are tertiary amine molecules that exist in an equilibrium between cationic (protonated) and neutral (unprotonated) forms. The neutral molecule can gain access to the key binding site in the channel pore (Ragsdale et al., 1996) by diffusing into the lipid membrane surrounding the channel and then entering the channel protein through “fenestrations” in the wall of the pore region (Payendah et al., 2011; Martin and Corry, 2014; Gamal El-Din et al., 2018; Nguyen et al., 2019), corresponding to the “hydrophobic pathway” proposed in a classic analysis of local anesthetic action (Hille, 1977). In a second “hydrophilic pathway” proposed in this analysis, the neutral form of the drug can diffuse across the membrane into the cytoplasm, where a fraction is re-protonated. From the cytoplasm, both cationic and neutral drug molecules can enter the channel to reach the binding site in the pore, but only when the channel is open. Consistent with this hypothesis, QX-314, a permanently charged quaternary analogue of lidocaine, cannot inhibit neuronal sodium channels when applied externally, but is effective when applied intracellularly (Frazier et al., 1970; Strichartz , 1973).

Although QX-314 cannot readily diffuse across the cell membrane, it can enter some neurons by permeating through certain cation-selective ion channels that have unusually large pores, notably TRPV1 and TRPA1 channels (Binshtok et al., 2007; Puopolo et al., 2013; Brenneis et al., 2014). Because these channels are selectively expressed in populations of nociceptive (pain-sensing) primary sensory neurons, application of QX-314 together with activators of TRPV1 or TRPA1 channels can produce selective inhibition of nociceptors with minimal inhibition of motor neurons or non-nociceptive sensory neurons, in contrast to the non-selective nerve block produced by lidocaine (Gerner et al., 2008; Binshtok et al., 2009; Kim et al., 2010; Roberson et al., 2011; Brenneis et al., 2013; Zhou et al., 2014).

Pain associated with tissue inflammation is mediated in part by activation of TRPV1 and TRPA1 channels in nociceptors (reviewed by Bautista et al., 2013; Julius, 2013), raising the possibility that endogenous activation of these channels might be sufficient to catalyze entry of QX-314 or other cationic sodium channel blockers in inflamed tissue, without requiring co-application with exogenous TRP activators. An especially intriguing possible application of the strategy is in cough, which is mediated by airway sensory neurons, including a population of nociceptors expressing TRPV1 and TRPA1 channels (Bonvini et

al., 2015; Canning et al., 2014; Mazzone and Undem, 2016). Inhaled lidocaine is used to inhibit reflexive laryngospasm and cough during bronchoscopy and is highly effective for acute suppression of cough in patients with upper respiratory tract infections (Peleg and Binyamin, 2002), COPD (Chong et al., 2005; Udezue, 2001), and asthma (Slaton et al., 2013; Udezue, 2001). However, lidocaine has a short duration of action (Chong et al., 2005) and produces potential cardiac and CNS side effects (Shirk et al., 2006) as a consequence of its high lipophilicity and ready diffusion into the bloodstream. Also, because lidocaine blocks activity in motor neurons as well as sensory neurons, it inhibits swallowing and the gag reflex (Noitasaeng et al., 2016), limiting its clinical utility.

Here, we have designed and synthesized a novel cationic compound, BW-031, with improved potency for inhibiting sodium channels compared to QX-314. We find that BW-031 when applied alone to inflamed tissue produces long-lasting inhibition of inflammatory pain in several rat and mouse models and that inhaled BW-031 can effectively inhibit cough in a guinea pig model of allergic airway inflammation.

Methods

Chemicals.

Except for BW-031, all chemicals were purchased from Sigma Aldrich or Tocris Bioscience. BW-031 (1-(1-(2, 6-dimethylphenylamino)-1-oxobutan-2-yl)-1-ethylpiperidinium) was synthesized by Acesys Pharmatech according to the pathway described in Supporting Information.

Stable cell line electrophysiology.

Human embryonic kidney (HEK 293) cells stably expressing the human $Na_v1.7$ channel (Liu et al., 2012) were grown in Minimum Essential Medium (MEM, ATCC) containing 10% fetal bovine serum (FBS, Sigma), penicillin/streptomycin (Sigma), and 800 μg/ml G418 (Sigma) under 5% CO_2 at 37°C. Human embryonic kidney (HEK 293) cells stably expressing the human $Na_v1.1$ channel (Kahlig et al., 2010; gift of Dr. Alfred L. George, Jr.) were grown in Dulbecco's Modified Eagle Medium (DMEM, Thermo Fisher Scientific) containing 10% FBS (Sigma), penicillin/streptomycin (Sigma), and 3 μg/ml Puromycin (Sigma) under 5% CO_2 at 37°C. Chinese Hamster Ovary (CHO-K1) cells stably expressing the human $Na_v1.8$ channel and beta3 subunit (B'SYS GmbH, Catalog CHO-NaV1.8/β3) were grown in Ham's F-12 medium (Corning) containing 10% FBS, penicillin/streptomycin (Sigma), and 3.5 μg/ml Puromycin (Sigma) and 350 μg/ml Hygromycin (Sigma) under 5% CO_2 at 37°C. For electrophysiological recordings, cells were re-plated on coverslips for 1 to 6 h before recording. Whole-cell recordings were obtained using patch pipettes with resistances of 2-2.5 MΩ when filled with the internal solution consisting of (in mM): 61 CsF, 61 CsCl, 9 NaCl, 1.8 $MgCl_2$, 9 EGTA, 14 creatine phosphate (tris salt), 4 MgATP, and 0.3 GTP (tris salt), 9 HEPES, pH adjusted to 7.2 with CsOH. The shank of the electrode was wrapped with Parafilm in order to reduce capacitance and allow optimal series resistance compensation without oscillation. Seals were obtained and the whole-cell configuration established with cells in Tyrode's solution consisting of (in mM): 155 NaCl, 3.5 KCl, 1.5 $CaCl_2$, 1 $MgCl_2$, 10 HEPES, 10 glucose, pH adjusted to 7.4 with NaOH. After establishing

whole-cell recording, cells were lifted off the bottom of the recording chamber and placed in front of an array of quartz flow pipes (250 μm internal diameter, 350 μm external diameter). Recordings were made using a base external solution of Tyrode's solution with added 10 mM TEA-Cl to inhibit small endogenous potassium currents. Solution changes were made (in < 1 second) by moving the cell between adjacent pipes. Currents were recorded at room temperature (21-23°C) with an Multiclamp 700B amplifier (Molecular Devices) and filtered at 5 kHz with a low-pass Bessel filter The amplifier was tuned for partial compensation of series resistance (typically 70-80% of a total series resistance of 4-10 MΩ), and tuning was periodically re-adjusted during the experiment. Currents were digitized using a Digidata 1322A data acquisition interface controlled by pCLAMP 9.2 software ([RRID:SCR_011323], Molecular Devices).

Human iPSC-derived nociceptor neuron electrophysiology.

Neurons were differentiated from human induced pluripotent stem cells (IPSCs) following a previous protocol that yields cells expressing peripherin and multiple markers of nociceptors, including expression of genes such as SCN10A and P2XR3 (Chambers et al., 2012). Cells were cultured in 35 mm dishes (Falcon), coated with 0.1 mg/ml poly-d-lysine (Sigma) and 10 μg/ml laminin, and grown in DMEM/F12(1:1) media (Life Technologies) containing 10% HI FBS (Life Technologies) and 35 μg/ml Ascorbic acid (Sigma), 10 ng/ml BDNF, 10 ng/ml GDNF, 10 ng/ml NGF, 10 ng/ml NT-3 (Life technologies) for 8 weeks. Whole-cell recordings were made using patch pipettes with resistances of 1.5-2.5 MΩ when filled with the internal solution consisting of (in mM): 140 CsF, 10 NaCl, 1.1 EGTA, 10 HEPES, 20 D-glucose, pH adjusted to 7.2 with CsOH. The external solution consisted of (in mM): 130 NaCl, 20 TEA-Cl, 5 KCl, 0.1 $CdCl_2$, 2 $CaCl_2$, 1 $MgCl_2$, 10 D-glucose, 10 HEPES, pH adjusted to 7.4 with NaOH, which was perfused during the recording using the ValveBank perfusion system (Automate Scientific). The size of neurons was measured with an inverted microscope (Nikon Eclipse Ti), and neurons with a diameter of less than 25 μm were used for the experiments. Currents were recorded using a Multiclamp 700B amplifier (Molecular Devices). Data were collected and digitized at 50 kHz using a Digidata 1440 16-bit A/D converter controlled by pCLAMP 10.5 software (Molecular Devices).

Electrophysiology data analysis.

Data were analyzed using programs written in IGOR Pro 6.0 ([RRID:SCR_000325], Wavemetrics, Lake Oswego, OR), using DataAccess (Bruxton Software) to read pCLAMP data files into Igor Pro. No correction was made in the reported voltage protocols for the liquid junction potential between the internal solution and the Tyrode's solution in which the pipette was zeroed. Currents were corrected for linear capacitive and leak currents, which were determined using 5 mV hyperpolarizations delivered from the resting potential and then appropriately scaled and subtracted. Statistical analyses were performed using IGOR Pro.

Mouse dorsal root ganglion (DRG) neuron culture and electrophysiology.

DRG neurons were cultured as previously described (Costigan et al., 1998). Animal use for culturing neurons complied with the ARRIVE guidelines (Percie du Sert et al., 2020) and with the recommendations made by the British Journal of Pharmacology (Lilley et

al., 2020), using the minimum number of animals to obtain the data. All procedures were approved by the Institutional Animal Care and Use Committee (IACUC), Boston Children's Hospital. Adult male C57Bl/6J mice (8-12 weeks old, Jackson Laboratories stock #000664 [RRID:IMSR_JAX:000664]) were euthanized by a slowly rising concentration of CO_2 and exsanguinated. DRGs were dissected from into Hank's balanced salt solution (HBSS) (Life Technologies). DRGs were dissociated in 1 μg/ml collagenase A plus 2.4 U/ml dispase II (enzymes, Roche Applied Sciences) in HEPES-buffered saline (HBSS, Sigma) for 90 min at 37 °C and then triturated down to single-cell level using glass Pasteur pipettes of decreasing size. DRGs were then centrifuged over a 10% BSA gradient and plated on laminin-coated cell culture dishes (Sigma). DRGs were cultured overnight in B27-supplemented neurobasal-A medium plus penicillin/streptomycin (Life Technologies). On the day following plating, DRG culture dishes were treated with either HBSS, 100 μM BW-031, 1 μM capsaicin or 100 μM BW-031+1 μM capsaicin in HBSS for 30 min, followed by a 5-minute perfusion of external solution to remove extracellular compounds.

Whole-cell current-clamp and voltage-clamp recordings were performed <24 hours after DRG culture using an Axopatch 200A amplifier (Molecular Devices) at 25°C. Data were sampled at 20 kHz and digitized with a Digidata 1440A A/D interface and recorded using pCLAMP 10 software (Molecular Devices). Data were low-pass filtered at 2 kHz. Patch pipettes were pulled from borosilicate glass capillaries on a Sutter Instruments P-97 puller and had resistances of 1.5–3 MΩ. Series resistance was 3–10 MΩ and compensated by at least 80% and leak currents were subtracted. Cells were classified as $TRPV1^+$ or $TRPV1^-$ by the presence or absence of a response to perfused 1 μM capsaicin measured in voltage clamp mode at a holding potential of −80 mV. Cells were then held at −100mV and depolarized to −10mV with a 100 ms step to activate Na_v channels. The external solution for DRG electrophysiological recordings consisted of (in mM): 30 NaCl, 90 Choline-Cl, 20 TEA-Cl, 3 KCl, 1 $CaCl_2$, 1 $MgCl_2$, 0.1 $CdCl_2$, 10 HEPES, 10 Dextrose; pH 7.4, 320 mOsm. The internal pipette solution consisted of (in mM): 140 CsF, 10 NaCl, 1 EGTA, 10 HEPES, 20 Dextrose; pH 7.3. No correction was made in the reported voltage protocols for the liquid junction potential between this solution and the external solution.

Animals for pain studies.

Animal use for pain studies comply with the ARRIVE guidelines (Percie du Sert et al., 2020) and with the recommendations made by the British Journal of Pharmacology (Lilley et al., 2020). Every effort was made to minimize animal suffering and the number of animals used. Experiments were designed to use the minimum number of animals to provide sufficient statistical power based on our previous experience with the behavioral assays, where variability within a group of wild type mice is approximately 10 and 20% of the mean.

Male CD rats (7-8 weeks old) were purchased from Charles River and male C57BL/6J mice (8-12 weeks old) were purchased from Jackson Laboratories (stock #000664 [RRID:IMSR_JAX:000664]) and housed for 1 week prior to experiments. Rats were housed 3 animals per cage and mice were housed 5 animals per cage in separate rooms with constant temperature (23°C) and humidity (45-55%) with food and water available *ad*

libitum. At the end of the experiments, animals were euthanized by inhalation of a slowly rising concentration of CO2 (30-70% over 5 minutes). All procedures were approved by the Institutional Animal Care and Use Committee (IACUC), Boston Children's Hospital.

Mice and rats were used for studies of pain because it enabled us to compare our results with a large body of work studying pain in rodent models and because there is no suitable in vitro, cellular, or computational model that can recapitulate the complexity of the neural substrates that result in the output of pain-related behavior and which could be used to assess *in vivo* biological function relevant to humans.

Male rats and mice were used for pain studies following previous practice in the lab, reflecting the widespread belief in the field that female subjects would introduce higher variability due to cycling gonadal hormones. It is now recognized that this assumption is likely incorrect and has introduced a deleterious bias in the scientific literature (Mogil, 2020) and that future studies should use equal numbers of male and female animals.

Plantar incision surgery.

Rats were placed in a chamber with 5% isoflurane and monitored until they were visibly unconscious. Once unconscious, rats were removed from the chamber and anesthesia was maintained using 2% isoflurane delivered via nose cone. A toe pinch was used to confirm that animals were fully anesthetized. The animals were then secured with surgical tape at their toes and upper leg for paw stability during surgery. The plantar surface of one hind paw was sterilized with 3 alternating wipes of betadine and ethanol. A 1.5 cm longitudinal incision was made using a scalpel along the center of the plantar surface, beginning 1 cm from the heel and extending towards the foot pad and toes. Incision was made to the minimal depth necessary to cut through skin and fascia to expose the underlying plantaris muscle, approximately 1-2 mm. Once exposed the plantaris muscle was elevated for 10 seconds with surgical forceps and gently lifted for 10 seconds. After irritation of the plantaris muscle, the wound was closed with three sutures. After surgery animals were returned to their cage and monitored until they fully recovered from anesthesia. Treatments were administered subcutaneously 24 hours after injury.

Intraplantar injection of Complete Freund's Adjuvant.

Complete Freund's Adjuvant (CFA) was purchased from Sigma Aldrich (Cat. No. F5881). Rats were restrained and subcutaneously injected in the plantar region of the left paw with 50 μL of CFA (1 mg/ml). Animals receiving test compounds (2% QX-314 or 2% BW-031) were injected with these compounds dissolved in 50 μL of CFA.

Plantar ultraviolet (UV) burn.

Mice were anesthetized with 3% isoflurane. UV irradiation was performed on the plantar surface of the left hind paw under maintenance anesthesia with 2% isoflurane at an intensity of 0.5 J/cm^2 for 1 minute at a wavelength of 305–315 nm using a fluorescent UV-B light source (XR UV LEDs 308nm, RayVio, Hayward, California, USA).

Peri-sciatic injection.

Mice were anesthetized with 2.5% isoflurane. Upon achieving sufficient depth of anesthesia, mice were placed in the prone position, the fur on their left hindleg was shaved and the area was cleaned with betadine and 70% isopropanol. A 1-centimeter incision was made in the skin on the upper thigh. The sciatic nerve was identified in the intermuscular interval between the biceps femoris and gluteal muscle without the dissection of the superficial fascia layers. Then, a mixture of physiological saline with 0.5% lidocaine, 0.5% QX-314 or 0.5% BW-031 (70 μL) was injected into the perineural space below the fascia using an insulin syringe with a 30-gauge needle. The surgical wounds were closed with stainless steel wound clips (EZ Clips, Stoelting Co.).

Behavioral measurements of sensory and motor function

Von Frey assay of mechanical sensitivity.—An electronic Von Frey device (Bioseb, Model: BIO-EVF4) was used to assess mechanical sensitivity in rats before and after paw incision injury. Animals were habituated for 1 hour, one day prior to baseline testing. Animals were given 30 minutes to settle before testing. An average mechanical threshold was calculated using 5 measurements taken 5 minutes apart for each animal. For baseline measurements two testing sessions were performed on separate days prior to injury and averaged together. 50 μL of BW-031 or saline were administered into the plantar region of the hind paw adjacent to the incision 24 hours post injury. Animals were then tested 1, 3, 5, and 24 hours post treatment. Additional timepoints were added at 7 and 9 hours for higher concentrations of treatments.

A manual Von Frey assay was used to assess mechanical sensitivity in mice before and after UV burn, as previously described (Lee et al., 2019). After mice were habituated to the testing cage (7.5 × 7.5 × 15 cm) with a metal grid floor for 45 min for 2 days, baseline values were measured using nine von Frey filaments with different bending forces (0.04, 0.07, 0.16, 0.4, 0.6, 1, 1.4, 2, and 4 g). The response patterns were collected and converted into corresponding 50% withdrawal thresholds using the Up-Down Reader software and associated protocol (Gonzalez-Cano et al., 2018). Based on the baseline measurement, mice were assigned to three groups so that the baseline mechanical sensitivity among the groups was similar. Each group consisted of 10 mice, based on previous experiments showing sufficient power to detect significance with 95% confidence. Twenty-four hours after UV irradiation, mice received a 10-μL bolus intraplantar injection of either 2% BW-031, 2% QX-314, or vehicle (normal saline) to the irradiated paw. The von Frey test was performed at 1, 3, 5, 7, and 24 hours after the drug injection.

Radiant heat assay of thermal sensitivity.—Thermal hypersensitivity was measured using the plantar radiant heat test (Hargreaves et al., 1988) (Ugo Basile, Model code: 37370) in CFA injected rats. Rats were habituated to testing enclosures for 1 hour one day prior to baseline testing. Rats were given 30 minutes to settle before testing. An average paw withdrawal latency was calculated using 3 measurements taken 5 minutes apart. Animals were tested 1, 4, and 24 hours after injury from CFA injection.

Toe spread assay of motor function.—Mouse toe movement was evaluated in the ipsilateral hind-paws as previously described (Ma et al., 2011) in order to assess the presence of motor block after peri-sciatic injection of lidocaine or charged sodium channel blockers. Briefly, 5 minutes after peri-sciatic injection, mice were lifted by the tail, uncovering the hind paws for clear observation. Under this condition, the digits spread, maximizing the space between them (the toe spreading reflex). This reflex was scored as previously described: 0, no spreading; 1, intermediate spreading with all toes; and 2, full spreading. Full toe spreading was defined as a complete, wide, and sustained (at least 2 seconds) spreading of the toes. Full toe spreading was observed in the contralateral paws for all mice tested.

Pinprick assay of sensory function.—Mouse responses to pinprick were measured as previously described (Ma et al., 2011), with modifications. Mice were placed in wire mesh cages and habituated for 3 sessions prior to peri-sciatic injection. After peri-sciatic injection and measurement of motor function, mice were immediately placed in wire mesh cages and an Austerlitz insect pin (size 000) (FST, USA) was gently applied to the plantar surface of the paw without moving the paw or penetrating the skin. The pinprick was applied three times to the sole of the ipsilateral hind paw and three times to the sole of the contralateral hind paw. A response was considered positive (1) when the animal briskly removed its paw. If none of the applications elicited a positive response, the overall grade was 0.

Blinding.—All behavioral measurements of sensory and motor function were performed by investigators blinded to the drug treatment; the test order was randomized with multiple groups being represented in each cage.

Guinea Pig Cough Experiments

Animals for guinea pig cough experiments.—Animal use for cough studies comply with the ARRIVE guidelines (Percie du Sert et al., 2020) and with the recommendations made by the British Journal of Pharmacology (Lilley et al., 2020). Every effort was made to minimize animal suffering and the number of animals used and studies were conducted in alignment with applicable animal welfare regulations in an AAALAC-accredited facility. The cough studies used 5-10 week-old Dunkin Hartley guinea pigs. The initial study using intratracheal application of BW-031 under isoflurane anesthesia used female animals (range of weights of 374-505 g on the day of dosing and cough challenge), with 9 animals per each of the 4 experimental groups. The choice of female guinea pigs was based on a previous belief in the laboratory that female guinea pigs are more susceptible to cough induction by citric acid, although research appearing since we did this study has now shown this belief to be false (Sterusky et al. Physiol Res 69:S171-179, 2020). The minimum number of animals was used in order to provide sufficient statistical power based on previous experiments on citric-acid induced cough in the laboratory. The subsequent study using ovalbumin sensitization to induce lung inflammation used 6 male (416-580 g) and 6 female (456-557 g) animals for each experimental group. There was no obvious difference between the initial cough numbers in male and female animals or in the inhibition of coughing by BW-031. The number of animals per group was increased in the ovalbumin sensitization experiments because of the expectation that variable levels of sensitization might increase variability

in the effectiveness with which BW-031 could enter nerve terminals. Because preliminary studies showed that some guinea pigs failed to cough in response to the citric acid challenge, each study began with 20% more animals than were planned for the protocols and animals were first pre-screened by inhalation of citric acid (400 mM for 7 minutes, with coughs counted during the 7 minute application and for 10 minutes afterward) and the lowest responders were omitted from the remaining study protocol. For the intratracheal protocol, animals with 0-1 coughs were omitted; for the ovalbumin sensitization protocol, the 6 animals of each sex with lowest cough counts (0-3 coughs) were omitted. Pre-screening was performed a minimum of 7 days before the start of the study protocol to allow animals to recover from any sensitization produced by the citric acid exposure during the pre-screening. After pre-screening, the remaining animals were allocated into each group so that each group had approximately equal group mean cough counts measured in the pre-screening protocol.

Intratracheal drug administration and citric acid challenge.—Animals were dosed via the intratracheal route at a dose volume of 0.5 mL/kg of BW-031 dissolved in saline based on individual bodyweights. Animals were anaesthetized (3-5% isoflurane/oxygen mix) and secured to the intubation device by a cord around their upper incisor teeth. A rodent fiber optic laryngoscope was inserted into the animal's mouth to illuminate the posterior pharynx and epiglottis. The tongue was released and the needle of the dosing device (Penn Century intratracheal aerosol Microsprayer) guided through the vocal cords into the lumen of the trachea. Following dosing, the animals were removed from the secured position and carefully monitored until full recovery. Approximately 1 hour after intratracheal treatment, animals were placed into whole body plethysmographs connected to a Buxco Finepointe System and exposed to nebulized 400 mM citric acid for 7 minutes. Cough counts were recorded during the 7 minute exposure period and for 10 minutes after nebulization period by the Buxco Finepointe system. Cough counts were recorded in an automated fashion by the Finepoint software, to remove any operator bias, with no involvement of the technician other than introducing the animal to the recording chamber. Recovery from the isoflurane anesthesia was complete within an hour based on the overt behavior of the animals, consistent with rapid recovery seen using measurements of physiological parameters (Schmitz et al., 2016).

Ovalbumin sensitization/challenge.—On Day 0 all animals were sensitized with intraperitoneal and subcutaneous injections of chicken egg albumin (ovalbumin). Animals were administered 1 mL of a 50 mg/mL Ovalbumin (Ova) in 0.9% w/v saline solution via the intraperitoneal route and 0.5 mL of the same solution into 2 separate subcutaneous sites (1 mL in total divided between the left and right flank). All animals were administered a single intraperitoneal dose of pyrilamine (15 mg/kg) at a dose volume of 1 mL/kg approximately 30 min prior to ovalbumin challenge on Day 14 to inhibit histamine-induced bronchospasm (Featherstone et al., 1988; Hara et al., 2005). On Day 14 animals were challenged with aerosolised ovalbumin in 0.9% w/v saline (3 mg/mL) or 0.9% w/v saline for 15 min. Animals were placed in groups in an acrylic box. 8 mL of ovalbumin in saline was placed in each of two jet nebulisers (Sidestream®). Compressed air at approximately

6 L/min was passed through each nebuliser and the output of the nebulisers passed into the box containing the animals.

Drug administration.—On Day 15 approximately 24 hours after the inflammatory challenge with ovalbumin, animals were placed in a whole-body plethysmograph (Buxco Finepointe) and dosed with vehicle or BW-031 by inhalation using an Aeroneb nebulizer (Aerogen) over 60 minutes. Upon the completion of dosing animals were returned to their home cage for approximately one hour before the cough challenge.

The inhaled dose of BW-031 was calculated according to the algorithm (Alexander et al., 2008): Inhaled dose (mg/kg) = [C (mg/L) x RMV (L/min) x D (min)]/BW (kg), where C is the concentration of drug in air inhaled, RMV is respiratory minute volume, D is the of exposure in minutes, BW is bodyweight in kg, with RMV (in L/min) calculated as 0.608 x BW $(kg)^{0.852}$.

Cough/respiratory function measurement.—One hour following the end of vehicle or drug administration on Day 15, the animals were placed into a whole-body plethysmograph connected to a Buxco Finepointe system. Animals were then exposed to nebulized 400 mM citric acid for 7 minutes. Cough counts were recorded throughout the 7 minute exposure period and for 10 minutes following the end of nebulization period. Animals were euthanized within approximately 60 min following the end of the cough challenge recording period by an overdose of pentobarbitone administered by the intraperitoneal route.

Tissue sampling.—Upon euthanasia, 2 mL of blood were sampled from the descending vena cava from each animal. The blood was allowed to stand at room temperature for a minimum of 60 minutes but less than 120 minutes to allow the clotting process to take place. Samples were then centrifuged at 2000 g for 10 minutes at 25°C and the resulting serum was frozen at −80°C for subsequent analysis of BW-031 concentrations. Also following termination an incision was made in the neck and the muscle layers were separated by blunt dissection and the trachea isolated. A small incision was made in the trachea and a tracheal cannula inserted. The cannula was secured in place with a piece of thread. The lungs were then removed and the left lung lobe tied off and removed. The right lung was lavaged with 3 mL of phosphate buffered saline (PBS) at room temperature. The PBS was left in the airway for 10 seconds whilst the organ was gently massaged before being removed, this was repeated twice further. In total, three lots of 3 mL of PBS was used to lavage the right lung.

BAL immune cell quantification.—A total and differential cell count of the BAL was performed using the XT-2000iV (Sysmex UK Ltd). The sample was vortexed for approximately 5 seconds and analyzed. A total and differential cell count (including eosinophils, neutrophils, lymphocytes and mononuclear cells (includes monocytes and macrophages)) was reported as number of cells per right lung per animal.

Liquid Chromatography/Mass Spectrometry (LC/MS).—Serum samples were kept at −80°C until being assayed, at which time they were thawed at room temperature. Each serum sample was added to 100 μL of 80:20 (acetonitrile:water) solution and the mixture

placed in a 1.5 mL Eppendorf Safe-Lock tubes prefilled with zirconium oxide beads (Next Advance Inc., Troy, NY). After vortexing for 30 seconds and sonicating for 10 minutes, the homogenate was centrifuged at 10,000 rpm for 10 minutes. The supernatant was then separated into a new Eppendorf tube to be stored at −80°C until the time for analysis. To 20 μL of liquid sample, 10 μL of internal standard (bupivacaine 10 ng/mL in acetonitrile:water (50:50)) were added, plus 170 μL of methanol chilled at 4°C. After vortexing for 30 seconds, the mixture was centrifuged at 10,000 rpm for 10 minutes. The supernatant solution was then transferred to a clean Eppendorf tube and evaporated to dryness under vacuum at 50 °C for 40 minutes. The residue was reconstituted with 100 μL of the starting mobile phase, i.e. aqueous 0.1% formic acid:methanol (90:10), and vortexed for 30 seconds. This solution was transferred to amber screw neck vials and setup in the refrigerated autosampler tray of the chromatograph for injection. This whole procedure was also applied to spiked calibrators and quality control QC samples used in the quantification and validation methods. At least three injections were carried out from each vial. Bupivacaine, used as internal standard, methanol LC/MS grade, and formic acid LC/MS grade were purchased from Sigma-Aldrich St. Louis, MO, USA). Pure MilliQ water at 18 MΩ-cm was obtained by reserve osmosis with a Direct-Q3 UV water purifier (Millipore SAS, France).

The quantification of BW-031 in serum fluid samples was carried out with an Acquity H Class UPLC chromatographer with a XEVO TQ MS triple quadrupole mass spectrometer detector (Water Corp., Milford, MA, USA). The assay used an Acquity UPLC BEH C18 1.7 μm 2.1x100 mm column with a VanGuard 2.1X 5 mm guard column, both kept at constant 35°C. The mobile phase was ran on a gradient of A: aqueous 0.1% formic acid and B: methanol starting at time zero with a A:B proportion of 90:10, at 3 min 10:90, and at 4.2 min 90:10 until the end of the run at 6 minutes. The flow rate was set at 0.3 mL/min, with an injection volume of 3 μL, and a post-run organic wash of 5 seconds. Multiple reaction monitoring (MRM) was used for the mass spectrometry acquisition in positive electrospray ionization (ESI) mode. The mass transitions monitored were m/z 263.22→86.02 and m/z 289.09→140.2, for BW-031 and bupivacaine respectively. The cone voltages were 36V and 30V, and the collision energies 24eV and 12eV, also respectively. The whole LC/MS system was controlled by the MassLynx v.4.2 software ([RRID:SCR_014271], Water Corp., Milford, MA, USA), including the TargetLynx Application Manager for data processing and analytes quantification. Good linearity and reproducibility were achieved in the range of 1–100 ng/mL, and the precision and accuracy of the method were 2.74% and 98.6%, respectively. The lower limit of quantification was 1.8 ng/mL.

Cardiotoxicity.—Frozen human IPSC-derived cardiomyocytes (Cor.4U cardiomyocytes, [RRID:CVCL_Y550]) were purchased from Axiogenesis AG (currently NCardia AG). Cor.4U cells were thawed and plated at a density of 10000 cells/well into 384-well plates that were pre-coated with 10 μg/mL bovine fibronectin in sterile phosphate buffered saline, pH 7.4. Cor.4U Culture Medium (Axiogenesis) was used to maintain the cells in culture for 7 days and was changed daily. Cells exhibited synchronous beating on day 3 after plating. On day 7 after plating, the medium was changed to BMCC medium (Axiogenesis). The EarlyTox Cardiotoxicity Kit (Molecular Devices) was used to measure calcium flux as a proxy for cardiomyocyte beating activity[112]. Cor.4U cells were incubated with the EarlyTox

calcium sensitive dye in BMCC media for 1 hour, and then the plates were transferred to the FDSS700EX plate reader (Hamamatsu Photonics). The baseline calcium flux was measured for 5 minutes and then charged local anesthetics dissolved in BMCC media or media alone were added to the wells using a robot. 10 minutes after compound treatment, the calcium flux was measured again. All measurements were performed at 37°C under 95% CO_2/5% O_2. Calcium flux parameters were measured using the Hamamatsu Analysis Software.

Data and statistical analysis

The data and statistical analysis comply with the recommendations of the British Journal of Pharmacology on experimental design and analysis in pharmacology (Curtis et al., 2018). Statistical analysis was carried out only for data where sample size was at least 5 for each group. All experimental data points including outliers were included in the scatter plots and data analysis. The analysis was carried out using GraphPad Prism 8 software ([RRID:SCR_002798], GraphPad Software Inc., San Diego, CA, USA). All data are expressed as the mean ± standard deviation (SD). Statistical comparisons were made using a paired two-tailed Student's t test for two groups or ANOVA for multiple groups, using the Kolmogorov–Smirnov test to evaluate normality and Bartlett and Brown–Forsythe tests for homogeneity of variance. Post hoc tests were conducted only if the F in ANOVA achieved $P< 0.05$, and there was no significant variance inhomogeneity. In most cases in which there was variance inhomogeneity (data in Figures 3A, 6B, 7B), we achieved homogeneity of variance by transforming raw data using logarithmic transformation prior to using ANOVA. The resulting Bartlett’s tests were non-significant indicating success of the transformation method. In a case (Figure 8A) in which several transforms could not be found to normalize the variance (as shown by significant Bartlett’s tests after each transform method), we employed non-parametric Kruskall Wallis ranks analysis. For experiments with repeated measurements (Figures 4 and 5), the Greenhouse-Geisser test was used to test for deviations from sphericity in the repeated-measurement experiments and in cases where a significant deviation occurred (Greenhouse-Geisser epsilon<0.99), the Greenhouse-Geisser correction was applied. Details of the statistical tests used for the data in each figure are given in Supporting Information. There is only one threshold for statistical significance ($P < 0.05$) in all analysis.

Nomenclature of Targets and Ligands

Key protein targets and ligands in this article are hyperlinked to corresponding entries in http://www.guidetopharmacology.org, the common portal for data from the IUPHAR/BPS Guide to PHARMACOLOGY (Harding et al., 2018), and are permanently archived in the Concise Guide to PHARMACOLOGY 2019/20 (Alexander et al., 2019).

Results

Among local anesthetics with an amino-amide scaffold like lidocaine, compounds like bupivacaine and mepivacaine in which the amino group is part of a piperidine ring have particularly high potency for sodium channel inhibition (Bräu et al., 1998; Scholz et al., 1998). Based on this, we designed and synthesized compounds containing a cationic charge in a piperidinium ring and identified one, BW-031 (Figure 1a), as a compound that

inhibited $Na_v1.7$ sodium channels with substantially higher potency than QX-314 when applied intracellularly (Figures 1b-c). As for QX-314 (Strichartz, 1973; Schwarz et al., 1977; Yeh, 1978), inhibition by BW-031 progressively accumulates with each cycle of activation and deactivation of the sodium channel, as if the intracellular blocker can enter the channel only when it is open and is effectively trapped within the channel after the channel closes. The currents remaining after partial inhibition by 30 μM BW-031 applied intracellularly had unchanged voltage-dependence of activation and a voltage-dependence of availability (assayed using 50-ms conditioning pulses) that was slightly shifted (~11 mV) in the hyperpolarizing direction (Supplementary Figure 1); a possible interpretation is that channels with BW-031 trapped inside are completely unable to pass current, so that the activation curve represents channels with no drug, but that the fraction of channels containing BW-031 can change during the 50-ms conditioning pulses, as if strong hyperpolarizations can to some extent “squeeze” BW-031 out of BW-031-containing channels. BW-031 had minimal effect on $Na_v1.7$ currents when applied extracellularly (Figures 1d-e), suggesting that, like QX-314, it cannot effectively enter sodium channels through the narrow ion selectivity filter in the outer pore region of the channel or diffuse across the cell membrane. Intracellular BW-031 inhibited native sodium currents in nociceptors differentiated from human induced pluripotent stem cells (hiPSCs) with very similar potency as for heterologously expressed $Na_v1.7$ channels (Figures 1f-g). Intracellular BW-031 inhibited $Na_v1.1$ channels with a similar potency to $Na_v1.7$ channels (Figures 2a,b). Intracellular BW-031 also inhibited heterologously-expressed $Na_v1.8$ channels (Figures 2c,d) but with greatly reduced potency compared to Nav1.7 and Nav1.1 channels, with intracellular 300 μM BW-031 producing 30±18% inhibition (mean±SD, n=5), similar to the effect of 3 μM BW-031 on $Na_v1.7$ channels (37±9% inhibition, n=6). The much weaker effect on $Na_v1.8$ channels was unexpected, because previous work showed that the uncharged piperidine-containing anesthetics bupivacaine and mepivacaine have generally similar effects on native TTX-resistant sodium channels in DRG neurons and heterologously-expressed $Na_v1.8$ channels as on a variety of TTX-sensitive channels (Bräu et al., 1998; Scholz et al., 1998; Scholz and Vogel, 2000; Leffler et al, 2010). Previous experiments with native Nav1.8 channels in rat DRG neurons showed ~30% use-dependent inhibition by internal 200 μM QX-314 with 0.75 Hz stimulation (Leffler et al., 2005) which by comparison with effects of 100 μM QX-314 on Nav1.7 channels (Figure 1b,c) raises the possibility that Nav1.8 channels may be less sensitive than Nav1.7 channels to inhibition by intracellular charged blockers in general, but more work will be required to examine this in detail.

BW-031 applied externally to mouse DRG neurons inhibited sodium currents only when it was applied together with capsaicin to activate TRPV1 channels (Figure 3a) and the combined application of BW-031 and capsaicin had no effect on sodium currents in DRG neurons lacking expression of TRPV1 channels, as tested by the response to 1 μM capsaicin (Figure 3b). Thus, like QX-314 (Binshtok et al., 2007; Brenneis et al., 2013, 2014; Stueber et al., 2016), BW-031 can permeate through activated TRPV1 channels to block sodium channels from the inside of the cell.

We next tested the possibility that BW-031 applied alone might be able to inhibit nociceptors in several rodent models of inflammatory pain. BW-031 effectively reduced hypersensitivity

in a rat model of inflammation induced by paw injection of Complete Freund's Adjuvant (CFA), in which inflammation activates TRPV1 and TRPA1 channels (Garrison and Stucky, 2014; Asgar et al., 2015; Kanai et al., 2007; Lennertz et al., 2012). In this model, latency of paw withdrawal to a thermal stimulus was decreased at 1 hour and even more at 4 hours, and BW-031 blocked this effect at both times (Figure 4a). Similarly, BW-031 also blocked mechanical hyperalgesia in a more clinically-relevant rat paw incision model of surgical pain (Brennan et al., 1996; Barabas and Stucky, 2013) in which the incision produced pronounced mechanical hyperalgesia when assayed 24 hours later. BW-031 injected near the incision greatly reduced the mechanical hyperalgesia, with strong effects at 3 hours and 5 hours after BW-031 injection that then progressively declined at later times (Figure 4b). Figure 5a shows results from a mouse model of UV-burn-induced inflammatory pain (Yin et al., 2016) where inflammatory mediators activate TRPV1 and TRPA1 channels in nociceptors (Acosta et al., 2014; Yin et al., 2016). Plantar UV-burn results in pronounced mechanical allodynia 24 hours later, at which time intra-plantar injection of 2% BW-031 produced robust mechanical analgesia lasting for at least 7 hours, with considerably longer-lasting effects than QX-314. Interestingly, in both the mouse UV burn model and the rat CFA paw-injection model, BW-031 not only reversed the tactile hypersensitivity resulting from the injury but also produced substantial long-lasting analgesia relative to the control situation, indicating a general inhibition of nociceptors at the site of administration to the inflamed tissue.

To test the selectivity of BW-031 to inhibit neurons only in conditions in which TRPV1, TRPA1 or other large-pore channels are activated, we performed perisciatic injections in naïve mice, with perisciatic injection of lidocaine as a positive control that inhibits neuronal activity without any requirement for activation of large-pore channels. We found that neither BW-031 nor QX-314 produced any block of either sensory or motor function, in contrast to the transient inhibition of both by lidocaine (Figures 5b,c), consistent with a requirement for activated TRP or other large-pore channels for neuronal inhibition by the charged blockers.

Guinea pigs are the standard pre-clinical model for studying cough (Adner et al., 2020; Bonvini et al., 2015; Lewis et al., 2007; Morice et al., 2007) as the main features of airway innervation are similar in guinea pigs and humans (West et al., 2015; Mazzone and Undem, 2016). Coughing in guinea pigs can be mediated both by a subset of bronchopulmonary C-fibers and by a distinct mechanically-sensitive and acid-sensitive subtype of myelinated airway mechanoreceptors (Canning, 2006; Canning et al., 2014; Canning et al., 2004; Chou et al., 2018; Mazzone et al., 2009; Mazzone and Undem, 2016). The neurons mediating the C-fiber pathway have strong expression of both TRPV1 and TRPA1 channels (Bonvini et al., 2015; Canning et al., 2014; Mazzone and Undem, 2016), and coughing in both guinea pigs and humans can be evoked by both TRPV1 agonists like capsaicin (Bonvini et al., 2015; Brozmanova et al., 2012; Kanezaki et al., 2012; Laude et al., 1993) and by TRPA1 agonists (Birrell et al., 2009; Bonvini et al., 2015; Kanezaki et al., 2012; Long et al., 2019). The importance of this population of TRPV1 and TRPA1-expressing neurons in at least some forms of cough suggested the possibility that loading charged sodium channel inhibitors into these neurons might inhibit cough.

We used two different experimental protocols to test whether BW-031 can inhibit cough in guinea pigs when applied under conditions in which TRPV1 and TRPA1 channels are likely to be activated. In the first, we delivered a small volume (0.5 mL/kg) of different doses of BW-031 intratracheally to animals under transient isoflurane anesthesia (Figure 6), relying on the ability of isoflurane to activate TRPV1 and TRPA1 channels (Matta et al., 2008; Kichko et al., 2015). One hour after the administration of BW-031, coughing was induced by inhalation of aerosolized citric acid, which induces a low rate of coughing (typically 0.5-1 cough/minute (Tanaka and Maruyama, 2005)), and coughs were measured using whole-body plethysmography. BW-031 produced a dose-dependent reduction in the number of coughs evoked by citric acid. Animals dosed with 7.53 mg/kg BW-031 had cough counts of 0.9±1.3 (n=9) in a 17-minute period, compared to 9.4±7.3 in control animals (n=9), with complete suppression of coughing in 5 of the 9 animals dosed with 7.53 mg/kg BW-031.

With these encouraging results, we next tested BW-031 in a potentially more translationally-relevant guinea pig model of ovalbumin-induced allergic airway inflammation, which produces activation and upregulation of both TRPV1 and TRPA1 channels in the airways (Liu et al., 2015; McLeod et al., 2006; Watanabe et al., 2008). Guinea pigs were sensitized by intraperitoneal and subcutaneous injections of ovalbumin (Figure 7a). Fourteen days later, inhaled ovalbumin induced allergic airway inflammation, reflected by increased immune cell counts in the bronchoalveolar lavage (BAL) measured one day after the ovalbumin-challenge (Figure 7b). Nebulized BW-031 was administered to restrained awake guinea pigs via snout-only inhalation chambers one day after the allergen challenge, and cough was then induced by citric acid one hour after the inhalation of BW-031. BW-031 strongly inhibited the citric acid-induced cough in a dose-dependent manner (Figure 7c). At the highest dose tested (17.6 mg/kg), BW-031 reduced cough counts over 17 minutes from 10±5.5 in control (n=12) to 2.2±3.1 with BW-031 (n=12), with complete suppression of cough in 7 of the 12 animals treated with BW-031.

The hydrophobicity of local anesthetics like lidocaine enables ready absorption from lung tissue into the blood. In principle, the absorption of cationic compounds like BW-031 might be expected to be much less. The highest dose of inhaled BW-031 (17.6 mg/kg) resulted in a serum concentration of 419±160 nM (n=12) (Figure 8a), far lower than the average serum level of ~15 μM (3.6 μg/mL) lidocaine measured following lidocaine spray anesthesia used for bronchoscopy (Labedzki et al., 1983). The serum concentration of BW-031 after aerosol inhalation was many orders of magnitude below the concentration at which any effect of BW-031 was seen on contraction of human IPSC-derived cardiomyocytes (3 mM; Figure 8b,c). Thus, inhaled BW-031 should have a high therapeutic index with regard to *in vivo* cardiotoxicity, which is a significant concern with inhaled lidocaine (Horáček and Vymazal, 2012).

Discussion

These results show that the piperidinium-containing cationic compound BW-031 is a highly effective use-dependent sodium channel inhibitor when introduced intracellularly, acting with about 6-fold greater potency than QX-314. Like QX-314 (Binshtok et al., 2007; Puopolo et al., 2013), BW-031 had no effect on sodium currents in DRG neurons if applied

in the absence of large-pore channel stimulation and in contrast to lidocaine, had no effect on nerve function when applied perisciatically in the absence of inflammation. Consistent with its greater intrinsic potency compared to QX-314, BW-031 produced more effective and longer-lasting inhibition of hypersensitivity in a mouse UV-burn model. The overall concordance of potency between the *in vitro* studies with cloned Nav1.7 channels and *in vivo* pain models suggests that future screening of novel compounds in this class can start with *in vitro* studies on cell lines, reducing the need for animal studies in the initial phases of drug discovery.

Both QX-314 and BW-031 applied alone to inflamed tissue were effective in inhibiting inflammatory pain, consistent with extensive evidence that tissue inflammation is associated with activation of TRPV1 and TRPA1 channels by endogenous activators (Bautista et al., 2013, Julius, 2013). Besides the models of incisional pain and UV burn we studied, the activation of TRPV1 and TRPA1 channels has been found in many other examples of inflammation, including models of colitis and inflammatory bowel disease (Zielińska et al. 2015, Utsumi et al., 2018; Csekő et al., 2019; Jain et al., 2020), dermatitis (Liu et al., 2013), cystitis (DeBerry et al., 2014) and pancreatitis (Schwartz et al., 2013). Thus, there may be many potential clinical applications of the strategy to inhibit inflammatory pain. An unfortunate limitation of our studies on pain is that we used only male rats and mice, reflecting a previously widespread belief in the field that female subjects might introduce higher variability due to cycling gonadal hormones (a belief now known to be misguided and likely deleterious to clinical translation of rodent research (Mogil, 2020)), so that we cannot be sure our results will generalize to females.

Cough may be a particularly attractive application of nerve silencing by entry of charged sodium channels blockers through large pore channels. TRPV1 and TRPA1 channels are expressed in many neurons mediating cough (Belvisi et al., 2011; Birrell et al., 2009; Bonvini et al., 2015; Brozmanova et al., 2012; Forsberg et al., 1988; Grace and Belvisi, 2011; Jia et al., 2002; Laude et al., 1993; Undem et al., 2002) and are likely to be activated in many conditions triggering cough, including airway inflammation (Bessac and Jordt, 2008; Choi et al., 2018; Talbot et al., 2015; Talbot et al., 2020) and respiratory viral infection (Zaccone et al., 2016). Expression of TRPV1 channels is increased in airways of patients with chronic persistent cough (Groneberg et al., 2004) and after respiratory viral infection (Omar et al., 2017). In addition, increasing evidence suggests an important role for channels containing P2X3 proteins for mediating cough. P2X3 channels are expressed on sensory neurons innervating the lungs (Kollarik et al., 2018; Kwong et al., 2008; Mazzone and Undem, 2016) and P2X3 inhibitors reduce cough in guinea pig models (Bonvini et al., 2015; Garceau and Chauret, 2019; Pelleg et al., 2019) and appear promising in recent human cough trials (Morice et al., 2019; Smith et al., 2017; Smith et al., 2020a,b; Dicpinigaitis et al., 2020). Interestingly, recent work has demonstrated that P2X3 receptors form large-pore channels capable of passing large cations (Harkat et al., 2017), similar to TRPV1 and TRPA1 pores. Thus, it is plausible that activated P2X3-containing channels, as well as TRPV1 and TRPA1 channels, might provide a pathway for entry of BW-031 into cough-mediating neurons. However further work will be needed to test directly whether BW-031 can pass through TRPA1 channels, as previously shown for QX-314 by both direct measurements of permeation (Brenneis et al., 2014) and functional effects when co-applied

with TRPA1 activators (Lennertz et al., 2012; Stueber et al., 2016; Yamaki et al., 2021), or through P2X3 channels.

The strategy of using activated large-pore channels to introduce charged sodium channel blockers inside sensory neurons should inhibit the activity of the neurons to all subsequent stimuli and may therefore have greater efficacy than targeting single receptors like TRPV1, TRPA1, and P2X3. Once cationic sodium channel inhibitors are loaded into a cell (concentrated by the negative intracellular potential), they will not readily diffuse out through the cell membrane and can produce effects lasting for many hours, as is the case for the analgesic effect of QX-314 (Binshtok et al., 2009; Gerner et al., 2008; Roberson et al., 2011) and as we find here for BW-031 inhibition of inflammatory pain (Figures 4,5).

Overall, the ability of BW-031 to inhibit cough adds to previous evidence that targeting peripheral nerve activity by sodium channel inhibition can be an effective strategy for inhibiting cough (Muroi et al., 2011; Sun et al., 2017; Kollarik et al., 2018; Brozmanova et al., 2019; Patil et al., 2019; Undem and Sun, 2020). Using cationic sodium channel inhibitors should have the advantage of limiting the inhibition of nerve activity only to those neurons that express large-pore channels, like TRPV1, TRPA1, and P2X3, and only under those conditions, such as inflammation or noxious irritation, where these channels are activated. In mice, silencing nociceptors by QX-314 can reduce lung inflammation induced by both ovalbumin and house dust mite sensitization (Talbot et al., 2015), consistent with a significant role of nociceptors in exacerbating inflammation by release of pro-inflammatory neuropeptides (Chiu et al., 2012; Talbot et al., 2015; Crosson et al., 2021), raising the possibility that BW-031 and other more potent charged sodium channel blockers have the potential to be disease-modifying in human allergic airway inflammation.

The citric acid model of guinea pig cough, although widely used, clearly has limitations for predicting drug efficacy in human disease, because while TRPV1 and TRPA1 inhibitors are reasonably effective in this model (Leung et al., 2007; Mukhopadhyay et al., 2014) this has not been replicated, so far, in patients (Khalid et al., 2014; Belvisi et al., 2017; European Medicines Agency, 2013). It would be useful in future studies to explore the efficacy of BW-031 in other modes of cough induction, such as hypo-osmotic solutions or direct mechanical stimulation, which may activate different populations of nerve fibers than citric acid (Chou et al., 2018; Morice et al., 2007).

Supplementary Material

Refer to Web version on PubMed Central for supplementary material.

Acknowledgements

We are grateful to Alyssa Grantham, Mary Kate Dornon, Yu Wang, Daniel Taub, Huan Wang and Lee Barrett for technical assistance, to the Boston Children’s Hospital PK-lab for assistance with LC/MS experiments, and to Ronald Blackman, James Ellis, and Richard Batycky for helpful discussions and suggestions. This work was supported by the National Institutes of Health National Institute of Neurological Diseases and Stroke [R35NS105076 (C.J.W.), R01NS036855 (B.P.B.), R01NS110860 (B.P.B.), R01HL122531 (B.D.L.)], the Department of Defense [W81XWH-15-1-0480 (C.J.W. & B.B.)], Boston Biomedical Innovation Center, the Blavatnik Biomedical Accelerator Fund, and the Boston Children’s Hospital’s Technology Development Fund.

Data Availability

The data that support the findings of this study are available from the corresponding author upon reasonable request.

Abbreviations

TRPV1	Transient receptor potential cation channel subfamily V member 1
TRPA1	Transient Receptor Potential Cation Channel Subfamily A Member 1

References

Acosta MC, Luna C, Quirce S, Belmonte C, and Gallar J (2014). Corneal Sensory Nerve Activity in an Experimental Model of UV Keratitis. Investigative Ophthalmology & Visual Science 55, 3403–3412. [PubMed: 24787567]

Adner M, Canning BJ, Meurs H, Ford W, Ramos Ramírez P, van den Berg MPM, Birrell MA, Stoffels E, Lundblad LKA, Nilsson GP, et al. (2020). Back to the future: re-establishing guinea pig in vivo asthma models. Clinical science (London, England : 1979) 134, 1219–1242.

Alexander DJ, Collins CJ, Coombs DW, Gilkison IS, Hardy CJ, Healey G, Karantabias G, Johnson N, Karlsson A, Kilgour JD, et al. (2008). Association of Inhalation Toxicologists (AIT) working party recommendation for standard delivered dose calculation and expression in non-clinical aerosol inhalation toxicology studies with pharmaceuticals. Inhalation toxicology 20, 1179–1189. [PubMed: 18802802]

Alexander SPH, Mathie A, Peters JA, Veale EL, Striessnig J, Kelly E, Armstrong JF, Faccenda E, Harding SD, Pawson AJ, Sharman JL, Southan C, Davies JA, CGTP Collaborators. (2019) THE CONCISE GUIDE TO PHARMACOLOGY 2019/20: Ion channels. Br J Pharmacol. 176:S142–S228. [PubMed: 31710715]

Asgar J, Zhang Y, Saloman JL, Wang S, Chung MK, and Ro JY (2015). The role of TRPA1 in muscle pain and mechanical hypersensitivity under inflammatory conditions in rats. Neuroscience 310, 206–215. [PubMed: 26393428]

Barabas ME, and Stucky CL (2013). TRPV1, but not TRPA1, in primary sensory neurons contributes to cutaneous incision-mediated hypersensitivity. Mol Pain 9: 9. [PubMed: 23497345]

Bautista DM, Pellegrino M, and Tsunozaki M (2013). TRPA1: A gatekeeper for inflammation. Annu Rev Physiol 75: 181–200. [PubMed: 23020579]

Belvisi MG, Birrell MA, Wortley MA, Maher SA, Satia I, Badri H, Holt K, Round P, McGarvey L, Ford J, et al. (2017). XEN-D0501, a Novel Transient Receptor Potential Vanilloid 1 Antagonist, Does Not Reduce Cough in Patients with Refractory Cough. American journal of respiratory and critical care medicine 196, 1255–1263. [PubMed: 28650204]

Belvisi MG, Dubuis E, and Birrell MA (2011). Transient receptor potential A1 channels: insights into cough and airway inflammatory disease. Chest 140, 1040–1047. [PubMed: 21972382]

Bessac BF, and Jordt S-E (2008). Breathtaking TRP channels: TRPA1 and TRPV1 in airway chemosensation and reflex control. Physiology (Bethesda) 23, 360–370. [PubMed: 19074743]

Binshtok AM, Bean BP, and Woolf CJ (2007). Inhibition of nociceptors by TRPV1-mediated entry of impermeant sodium channel blockers. Nature 449, 607–610. [PubMed: 17914397]

Binshtok Alexander M., Gerner P, Oh Seog B., Puopolo M, Suzuki S, Roberson David P., Herbert T, Wang C-F, Kim D, Chung G, et al. (2009a). Coapplication of Lidocaine and the Permanently Charged Sodium Channel Blocker QX-314 Produces a Long-lasting Nociceptive Blockade in Rodents. Anesthesiology 111, 127–137. [PubMed: 19512868]

Birrell MA, Belvisi MG, Grace M, Sadofsky L, Faruqi S, Hele DJ, Maher SA, Freund-Michel V, and Morice AH (2009). TRPA1 agonists evoke coughing in guinea pig and human volunteers. American journal of respiratory and critical care medicine 180, 1042–1047. [PubMed: 19729665]

Bonvini SJ, Birrell MA, Smith JA, and Belvisi MG (2015). Targeting TRP channels for chronic cough: from bench to bedside. Naunyn-Schmiedeberg's archives of pharmacology 388, 401–420.

Bräu ME, Vogel W, and Hempelmann G (1998). Fundamental properties of local anesthetics: half-maximal blocking concentrations for tonic block of Na+ and K+ channels in peripheral nerve. Anesthesia and analgesia 87, 885–889. [PubMed: 9768788]

Brennan TJ, Vandermeulen EP, and Gebhart GF (1996). Characterization of a rat model of incisional pain. Pain 64, 493–501. [PubMed: 8783314]

Brenneis C, Kistner K, Puopolo M, Jo S, Roberson D, Sisignano M, Segal D, Cobos EJ, Wainger BJ, Labocha S, et al. (2014). Bupivacaine-induced cellular entry of QX-314 and its contribution to differential nerve block. British journal of pharmacology 171, 438–451. [PubMed: 24117225]

Brenneis C, Kistner K, Puopolo M, Segal D, Roberson D, Sisignano M, Labocha S, Ferreiros N, Strominger A, Cobos EJ, et al. (2013). Phenotyping the function of TRPV1-expressing sensory neurons by targeted axonal silencing. The Journal of neuroscience : the official journal of the Society for Neuroscience 33, 315–326. [PubMed: 23283344]

Brozmanova M, Mazurova L, Ru F, Tatar M, and Kollarik M (2012). Comparison of TRPA1-versus TRPV1-mediated cough in guinea pigs. European journal of pharmacology 689, 211–218. [PubMed: 22683866]

Brozmanova M, Svajdova S, Pavelkova N, Muroi Y, Undem BJ, and Kollarik M (2019). The voltage-gated sodium channel Na(V)1.8 blocker A-803467 inhibits cough in the guinea pig. Respiratory physiology & neurobiology 270, 103267. [PubMed: 31398537]

Canning BJ (2006). Anatomy and neurophysiology of the cough reflex: ACCP evidence-based clinical practice guidelines. Chest 129, 33s–47s. [PubMed: 16428690]

Canning BJ, Chang AB, Bolser DC, Smith JA, Mazzone SB, and McGarvey L (2014). Anatomy and neurophysiology of cough: CHEST Guideline and Expert Panel report. Chest 146, 1633–1648. [PubMed: 25188530]

Canning BJ, Mazzone SB, Meeker SN, Mori N, Reynolds SM, and Undem BJ (2004). Identification of the tracheal and laryngeal afferent neurones mediating cough in anaesthetized guinea-pigs. The Journal of physiology 557, 543–558. [PubMed: 15004208]

Chambers SM, Qi Y, Mica Y, Lee G, Zhang XJ, Niu L, Bilsland J, Cao L, Stevens E, Whiting P, et al. (2012). Combined small-molecule inhibition accelerates developmental timing and converts human pluripotent stem cells into nociceptors. Nature biotechnology 30, 715–720.

Chiu IM, von Hehn CA , and Woolf CJ (2012). Neurogenic inflammation and the peripheral nervous system in host defense and immunopathology. Nat Neurosci 15: 1063–1067. [PubMed: 22837035]

Choi JY, Lee HY, Hur J, Kim KH, Kang JY, Rhee CK, and Lee SY (2018). TRPV1 Blocking Alleviates Airway Inflammation and Remodeling in a Chronic Asthma Murine Model. Allergy, asthma & immunology research 10, 216–224.

Chong CF, Chen CC, Ma HP, Wu YC, Chen YC, and Wang TL (2005). Comparison of lidocaine and bronchodilator inhalation treatments for cough suppression in patients with chronic obstructive pulmonary disease. Emergency medicine journal : EMJ 22, 429–432. [PubMed: 15911951]

Chou Y-L, Mori N, and Canning BJ (2018). Opposing effects of bronchopulmonary C-fiber subtypes on cough in guinea pigs. American Journal of Physiology-Regulatory, Integrative and Comparative Physiology 314, R489–R498.

Costigan M, Mannion RJ, Kendall G, Lewis SE, Campagna JA, Coggeshall RE, Meridith-Middleton J, Tate S, and Woolf CJ (1998). Heat shock protein 27: developmental regulation and expression after peripheral nerve injury. The Journal of neuroscience : the official journal of the Society for Neuroscience 18, 5891–5900. [PubMed: 9671676]

Crosson T, Wang J-C, Doyle B, Merrison H, Balood M, Parrin A, et al. (2021). FcεR1-expressing nociceptors trigger allergic airway inflammation. J Allergy Clin Immunol. 1 13:S0091-6749(21)00008-7. doi: 10.1016/j.jaci.2020.12.644. Online ahead of print

Csekő K, Beckers B, Keszthelyi D, and Helyes Z (2019). Role of TRPV1 and TRPA1 Ion Channels in Inflammatory Bowel Diseases: Potential Therapeutic Targets? Pharmaceuticals (Basel) 12: 48.

Curtis MJ, Alexander S, Cirino G, Docherty JR, George CH, Giembycz MA, et al. (2018). Experimental design and analysis and their reporting II: updated and simplified guidance for authors and peer reviewers. Br J Pharmacol 175: 987–993. [PubMed: 29520785]

DeBerry JJ, Schwartz ES, and Davis BM (2014). TRPA1 mediates bladder hyperalgesia in a mouse model of cystitis. Pain 155: 1280–1287. [PubMed: 24704367]

Dicpinigaitis PV, McGarvey LP, and Canning BJ (2020). P2X3-Receptor Antagonists as Potential Antitussives: Summary of Current Clinical Trials in Chronic Cough. Lung 198, 609–616. [PubMed: 32661659]

European Medicines Agency (2013). A Phase 2a, Multi-Centre, Randomised, Double-Blind, Parallel Group, Placebo-Controlled Study to Evaluate Efficacy, Safetyand Tolerability of Inhaled GRC 17536, Administered for 4 Weeks, in Patientswith Refractory Chronic Cough. EU Clinical Trials Registry 2016.

Featherstone RL, Hutson PA, Holgate ST, and Church MK (1988). Active sensitization of guinea-pig airways in vivo enhances in vivo and in vitro responsiveness. The European respiratory journal 1, 839–845. [PubMed: 3229483]

Forsberg K, Karlsson JA, Theodorsson E, Lundberg JM, and Persson CG (1988). Cough and bronchoconstriction mediated by capsaicin-sensitive sensory neurons in the guinea-pig. Pulmonary pharmacology 1, 33–39. [PubMed: 2980286]

Frazier DT, Narahashi T, and Yamada M (1970). The site of action and active form of local anesthetics. II. Experiments with quaternary compounds. J Pharmacol Exp Ther 171: 45–51. [PubMed: 5410937]

Gamal El-Din TM, Lenaeus MJ, Zheng N, and Catterall WA (2018). Fenestrations control resting-state block of a voltage-gated sodium channel. Proc Natl Acad Sci U S A 115: 13111–13116. [PubMed: 30518562]

Garrison SR, and Stucky CL (2014). Contribution of transient receptor potential ankyrin 1 to chronic pain in aged mice with complete Freund's adjuvant-induced arthritis. Arthritis Rheumatol 66: 2380–2390. [PubMed: 24891324]

Garceau D, and Chauret N (2019). BLU-5937: A selective P2X3 antagonist with potent anti-tussive effect and no taste alteration. Pulm Pharmacol Ther 56, 56–62. [PubMed: 30902655]

Gerner P, Binshtok AM, Wang CF, Hevelone ND, Bean BP, Woolf CJ, and Wang GK (2008). Capsaicin combined with local anesthetics preferentially prolongs sensory/nociceptive block in rat sciatic nerve. Anesthesiology 109, 872–878. [PubMed: 18946300]

Gonzalez-Cano R, Boivin B, Bullock D, Cornelissen L, Andrews N, and Costigan M (2018). Up-Down Reader: An Open Source Program for Efficiently Processing 50% von Frey Thresholds. Frontiers in pharmacology 9, 433. [PubMed: 29765323]

Grace MS, and Belvisi MG (2011). TRPA1 receptors in cough. Pulm Pharmacol Ther 24, 286–288. [PubMed: 21074632]

Groneberg DA, Niimi A, Dinh QT, Cosio B, Hew M, Fischer A, and Chung KF (2004). Increased expression of transient receptor potential vanilloid-1 in airway nerves of chronic cough. American journal of respiratory and critical care medicine 170, 1276–1280. [PubMed: 15447941]

Hara J, Fujimura M, Myou S, Oribe Y, Furusho S, Kita T, Katayama N, Abo M, Ohkura N, Herai Y, et al. (2005). Comparison of cough reflex sensitivity after an inhaled antigen challenge between actively and passively sensitized guinea pigs. Cough 1, 6–6. [PubMed: 16270933]

Harding SD, Sharman JL, Faccenda E, Southan C, Pawson AJ, Ireland S, Gray AJG, Bruce L, Alexander SPH, Anderton S, Bryant C, Davenport AP, Doerig C, Fabbro D, Levi-Schaffer F, Spedding M, Davies JA, NC-IUPHAR (2018). The IUPHAR/BPS Guide to PHARMACOLOGY in 2018: updates and expansion to encompass the new guide to IMMUNOPHARMACOLOGY. Nucleic Acids Res. 46, D1091–1106. [PubMed: 29149325]

Hargreaves K, Dubner R, Brown F, Flores C, and Joris J (1988). A new and sensitive method for measuring thermal nociception in cutaneous hyperalgesia. Pain 32, 77–88. [PubMed: 3340425]

Harkat M, Peverini L, Cerdan AH, Dunning K, Beudez J, Martz A, Calimet N, Specht A, Cecchini M, Chataigneau T, et al. (2017). On the permeation of large organic cations through the pore of ATP-gated P2X receptors. Proceedings of the National Academy of Sciences of the United States of America 114, E3786–e3795. [PubMed: 28442564]

Hille B (1977). Local anesthetics: hyrophilic and hydrophobic pathways for the drug-receptor reaction. The Journal of General Physiology 69,497–515. [PubMed: 300786]

Horáček M, and Vymazal T (2012). Lidocaine not so innocent: Cardiotoxicity after topical anaesthesia for bronchoscopy. Indian J Anaesth 56, 95–96. [PubMed: 22529438]

Jain P, Materazzi S, De Logu F, Rossi Degl'Innocenti D, Fusi C, Li Puma S, et al. (2020). Transient receptor potential ankyrin 1 contributes to somatic pain hypersensitivity in experimental colitis. Sci Rep 10: 8632. [PubMed: 32451393]

Jia Y, McLeod RL, Wang X, Parra LE, Egan RW, and Hey JA (2002). Anandamide induces cough in conscious guinea-pigs through VR1 receptors. British journal of pharmacology 137, 831–836. [PubMed: 12411414]

Julius D (2013). TRP channels and pain. Annual review of cell and developmental biology 29, 355–384.

Kanai Y, Hara T, Imai A, and Sakakibara A (2007). Differential involvement of TRPV1 receptors at the central and peripheral nerves in CFA-induced mechanical and thermal hyperalgesia. Journal of Pharmacy and Pharmacology 59, 733–738. [PubMed: 17524240]

Kanezaki M, Ebihara S, Gui P, Ebihara T, and Kohzuki M (2012). Effect of cigarette smoking on cough reflex induced by TRPV1 and TRPA1 stimulations. Respiratory medicine 106, 406–412. [PubMed: 22209625]

Khalid S, Murdoch R, Newlands A, Smart K, Kelsall A, Holt K, Dockry R, Woodcock A, and Smith JA (2014). Transient receptor potential vanilloid 1 (TRPV1) antagonism in patients with refractory chronic cough: a double-blind randomized controlled trial. The Journal of allergy and clinical immunology 134, 56–62. [PubMed: 24666696]

Kahlig KM, Saridey SK, Kaja A, Daniels MA, George AL Jr, Wilson MH (2010) Multiplexed transposon-mediated stable gene transfer in human cells. Proc Natl Acad Sci USA. 107:1343–1348. [PubMed: 20080581]

Kichko TI, Niedermirtl F, Leffler A, and Reeh PW (2015). Irritant volatile anesthetics induce neurogenic inflammation through TRPA1 and TRPV1 channels in the isolated mouse trachea. Anesth Analg 120: 467–471. [PubMed: 25517196]

Kim HY, Kim K, Li HY, Chung G, Park C-K, Kim JS, et al. (2010). Selectively targeting pain in the trigeminal system. Pain 150: 29–40. [PubMed: 20236764]

Kollarik M, Sun H, Herbstsomer RA, Ru F, Kocmalova M, Meeker SN, and Undem BJ (2018). Different role of TTX-sensitive voltage-gated sodium channel (NaV1) subtypes in action potential initiation and conduction in vagal airway nociceptors. The Journal of Physiology 596, 1419–1432. [PubMed: 29435993]

Kwong K, Kollarik M, Nassenstein C, Ru F, and Undem BJ (2008). P2X2 receptors differentiate placodal vs. neural crest C-fiber phenotypes innervating guinea pig lungs and esophagus. American journal of physiology Lung cellular and molecular physiology 295, L858–865. [PubMed: 18689601]

Labedzki L, Ochs HR, Abernethy DR, and Greenblatt DJ (1983). Potentially toxic serum lidocaine concentrations following spray anesthesia for bronchoscopy. Klin Wochenschr 61: 379–380. [PubMed: 6865269]

Laude EA, Higgins KS, and Morice AH (1993). A comparative study of the effects of citric acid, capsaicin and resiniferatoxin on the cough challenge in guinea-pig and man. Pulmonary pharmacology 6, 171–175. [PubMed: 8219571]

Lee S, Jo S, Talbot S, Zhang HB, Kotoda M, Andrews NA, Puopolo M, Liu PW, Jacquemont T, Pascal M, et al. (2019). Novel charged sodium and calcium channel inhibitor active against neurogenic inflammation. eLife 8. e48118. [PubMed: 31765298]

Leffler A, Herzog RI, Dib-Hajj SD, Waxman SG, and Cummins TR (2005). Pharmacological properties of neuronal TTX-resistant sodium channels and the role of a critical serine pore residue. Pflugers Arch 451: 454–463. [PubMed: 15981012]

Leffler A, Reckzeh J, Nau C. (2010) Block of sensory neuronal Na+ channels by the secreolytic ambroxol is associated with an interaction with local anesthetic binding sites. Eur J Pharmacol. 630:19–28. [PubMed: 20044988]

Lennertz RC, Kossyreva EA, Smith AK, and Stucky CL (2012). TRPA1 mediates mechanical sensitization in nociceptors during inflammation. PloS one 7, e43597. [PubMed: 22927999]

Leung SY, Niimi A, Williams AS, Nath P, Blanc F-X, Dinh QT, and Chung KF (2007). Inhibition of citric acid-and capsaicin-induced cough by novel TRPV-1 antagonist, V112220, in guinea-pig. Cough 3, 1–5. [PubMed: 17210085]

Lewis CA, Ambrose C, Banner K, Battram C, Butler K, Giddings J, Mok J, Nasra J, Winny C, and Poll C (2007). Animal models of cough: literature review and presentation of a novel cigarette smoke-enhanced cough model in the guinea-pig. Pulm Pharmacol Ther 20, 325–333. [PubMed: 17240178]

Lilley E, Stanford SC, Kendall DE, Alexander SPH, Cirino G, Docherty JR, et al. (2020). ARRIVE 2.0 and the British Journal of Pharmacology: Updated guidance for 2020. Br J Pharmacol 177: 3611–3616. [PubMed: 32662875]

Liu B, Escalera J, Balakrishna S, Fan L, Caceres AI, Robinson E, et al. (2013). TRPA1 controls inflammation and pruritogen responses in allergic contact dermatitis. FASEB J 27: 3549–3563. [PubMed: 23722916]

Liu P, Jo S, and Bean BP (2012). Modulation of neuronal sodium channels by the sea anemone peptide BDS-I. Journal of neurophysiology 107, 3155–3167. [PubMed: 22442564]

Liu Z, Hu Y, Yu X, Xi J, Fan X, Tse C-M, Myers AC, Pasricha PJ, Li X, and Yu S (2015). Allergen challenge sensitizes TRPA1 in vagal sensory neurons and afferent C-fiber subtypes in guinea pig esophagus. Am J Physiol Gastrointest Liver Physiol 308, G482–G488. [PubMed: 25591867]

Long L, Yao H, Tian J, Luo W, Yu X, Yi F, Chen Q, Xie J, Zhong N, Chung KF, et al. (2019). Heterogeneity of cough hypersensitivity mediated by TRPV1 and TRPA1 in patients with chronic refractory cough. Respiratory research 20, 112. [PubMed: 31170994]

Ma CH, Omura T, Cobos EJ, Latremoliere A, Ghasemlou N, Brenner GJ, van Veen E, Barrett L, Sawada T, Gao F, et al. (2011). Accelerating axonal growth promotes motor recovery after peripheral nerve injury in mice. The Journal of clinical investigation 121, 4332–4347. [PubMed: 21965333]

Martin LJ, and Corry B (2014). Locating the route of entry and binding sites of benzocaine and phenytoin in a bacterial voltage gated sodium channel. PLoS Comput Biol 10: e1003688. [PubMed: 24992293]

Matta JA, Cornett PM, Miyares RL, Abe K, Sahibzada N, and Ahern GP (2008). General anesthetics activate a nociceptive ion channel to enhance pain and inflammation. Proc Natl Acad Sci U S A 105: 8784–8789. [PubMed: 18574153]

Mazzone SB, Reynolds SM, Mori N, Kollarik M, Farmer DG, Myers AC, and Canning BJ (2009). Selective expression of a sodium pump isozyme by cough receptors and evidence for its essential role in regulating cough. The Journal of neuroscience : the official journal of the Society for Neuroscience 29, 13662–13671. [PubMed: 19864578]

Mazzone SB, and Undem BJ (2016). Vagal Afferent Innervation of the Airways in Health and Disease. Physiological reviews 96, 975–1024. [PubMed: 27279650]

McLeod RL, Fernandez X, Correll CC, Phelps TP, Jia Y, Wang X, and Hey JA (2006). TRPV1 antagonists attenuate antigen-provoked cough in ovalbumin sensitized guinea pigs. Cough 2, 10–10. [PubMed: 17173683]

Mogil JS (2020). Qualitative sex differences in pain processing: emerging evidence of a biased literature. Nat Rev Neurosci 21: 353–365. [PubMed: 32440016]

Morice AH, Fontana GA, Belvisi MG, Birring SS, Chung KF, Dicpinigaitis PV, Kastelik JA, McGarvey LP, Smith JA, Tatar M, et al. (2007). ERS guidelines on the assessment of cough. European Respiratory Journal 29, 1256.

Morice AH, Kitt MM, Ford AP, Tershakovec AM, Wu W-C, Brindle K, Thompson R, Thackray-Nocera S, and Wright C (2019). The Effect of Gefapixant, a P2X3 antagonist, on Cough Reflex Sensitivity: A randomised placebo-controlled study. European Respiratory Journal, 1900439.

Mukhopadhyay I, Kulkarni A, Aranake S, Karnik P, Shetty M, Thorat S, Ghosh I, Wale D, Bhosale V, and Khairatkar-Joshi N (2014). Transient receptor potential ankyrin 1 receptor activation in vitro and in vivo by pro-tussive agents: GRC 17536 as a promising anti-tussive therapeutic. PloS one 9, e97005. [PubMed: 24819048]

Muroi Y, Ru F, Kollarik M, Canning BJ, Hughes SA, Walsh S, Sigg M, Carr MJ, and Undem BJ (2011). Selective silencing of NaV1. 7 decreases excitability and conduction in vagal sensory neurons. The Journal of physiology 589, 5663–5676. [PubMed: 22005676]

Nguyen PT, DeMarco KR, Vorobyov I, Clancy CE, and Yarov-Yarovoy V (2019). Structural basis for antiarrhythmic drug interactions with the human cardiac sodium channel. Proc Natl Acad Sci U S A 116: 2945–2954. [PubMed: 30728299]

Noitasaeng P, Vichitvejpaisal P, Kaosombatwattana U, Tassanee J, and Suwannee S (2016). Comparison of Spraying and Nebulized Lidocaine in Patients Undergoing Esophago-Gastro-Duodenoscopy: A Randomized Trial. Journal of the Medical Association of Thailand = Chotmaihet thangphaet 99, 462–468. [PubMed: 27501598]

Omar S, Clarke R, Abdullah H, Brady C, Corry J, Winter H, Touzelet O, Power UF, Lundy F, McGarvey LP, et al. (2017). Respiratory virus infection up-regulates TRPV1, TRPA1 and ASICS3 receptors on airway cells. PloS one 12, e0171681. [PubMed: 28187208]

Patil MJ, Sun H, Ru F, Meeker S, and Undem BJ (2019). Targeting C-fibers for peripheral acting anti-tussive drugs. Pulmonary Pharmacology & Therapeutics 56, 15–19. [PubMed: 30872160]

Payandeh J, Scheuer T, Zheng N, and Catterall WA (2011). The crystal structure of a voltage-gated sodium channel. Nature 475: 353–358. [PubMed: 21743477]

Peleg R, and Binyamin L (2002). Practice tips. Treating persistent cough. Try a nebulized mixture of lidocaine and bupivacaine. Canadian family physician Medecin de famille canadien 48, 275. [PubMed: 11889886]

Pelleg A, Xu F, Zhuang J, Undem B, and Burnstock G (2019). DT-0111: a novel drug-candidate for the treatment of COPD and chronic cough. Therapeutic advances in respiratory disease 13, 1753466619877960. [PubMed: 31558105]

Percie du Sert N, Hurst V, Ahluwalia A, Alam S, Avey MT, Baker M, et al. (2020). The ARRIVE guidelines 2.0: updated guidelines for reporting animal research. J Physiol 598: 3793–3801. [PubMed: 32666574]

Puopolo M, Binshtok AM, Yao GL, Oh SB, Woolf CJ, and Bean BP (2013). Permeation and block of TRPV1 channels by the cationic lidocaine derivative QX-314. Journal of neurophysiology 109, 1704–1712. [PubMed: 23303863]

Ragsdale DS, McPhee JC, Scheuer T, and Catterall WA (1996). Common molecular determinants of local anesthetic, antiarrhythmic, and anticonvulsant block of voltage-gated Na+ channels. Proceedings of the National Academy of Sciences of the United States of America 93: 9270–9275. [PubMed: 8799190]

Roberson DP, Binshtok AM, Blasl F, Bean BP, and Woolf CJ (2011). Targeting of sodium channel blockers into nociceptors to produce long-duration analgesia: a systematic study and review. British journal of pharmacology 164, 48–58. [PubMed: 21457220]

Schmitz S, Tacke S, Guth B, and Henke J (2016). Comparison of Physiological Parameters and Anaesthesia Specific Observations during Isoflurane, Ketamine-Xylazine or Medetomidine-Midazolam-Fentanyl Anaesthesia in Male Guinea Pigs. PloS one 11, e0161258. [PubMed: 27658033]

Scholz A, Kuboyama N, Hempelmann G, and Vogel W (1998). Complex blockade of TTX-resistant Na+ currents by lidocaine and bupivacaine reduce firing frequency in DRG neurons. Journal of neurophysiology 79, 1746–1754. [PubMed: 9535944]

Scholz A, and Vogel W (2000) Tetrodotoxin-resistant action potentials in dorsal root ganglion neurons are blocked by local anesthetics. Pain 89:47–52.. [PubMed: 11113292]

Schwartz ES, La J-H, Scheff NN, Davis BM, Albers KM, and Gebhart GF (2013). TRPV1 and TRPA1 antagonists prevent the transition of acute to chronic inflammation and pain in chronic pancreatitis. J Neurosci 33: 5603–5611. [PubMed: 23536075]

Schwarz W, Palade PT, Hille B. (1977) Local anesthetics. Effect of pH on use-dependent block of sodium channels in frog muscle. Biophys J. 1977

Shirk MB, Donahue KR, and Shirvani J (2006). Unlabeled uses of nebulized medications. American journal of health-system pharmacy : AJHP : official journal of the American Society of Health-System Pharmacists 63, 1704–1716. [PubMed: 16960254]

Slaton RM, Thomas RH, and Mbathi JW (2013). Evidence for therapeutic uses of nebulized lidocaine in the treatment of intractable cough and asthma. The Annals of pharmacotherapy 47, 578–585. [PubMed: 23548650]

Smith JA, Kitt MM, Butera P, Smith SA, Li Y, Xu ZJ, Holt K, Sen S, Sher MR, and Ford AP (2020a). Gefapixant in two randomised dose-escalation studies in chronic cough. European Respiratory Journal, 1901615.

Smith JA, Kitt MM, Morice AH, Birring SS, McGarvey LP, Sher MR, and Ford AP (2017). MK-7264, a P2X3 Receptor Antagonist, Reduces Cough Frequency in Patients with Refractory Chronic Cough: Results from a Randomized, Controlled, Phase 2b Clinical Trial. In B14 CLINICAL TRIALS ACROSS PULMONARY DISEASE (American Thoracic Society), pp. A7608–A7608.

Smith JA, Kitt MM, Morice AH, Birring SS, McGarvey LP, Sher MR, Li YP, Wu WC, Xu ZJ, Muccino DR, et al. (2020b). Gefapixant, a P2X3 receptor antagonist, for the treatment of refractory or unexplained chronic cough: a randomised, double-blind, controlled, parallel-group, phase 2b trial. The Lancet Respiratory medicine 8, 775–785. [PubMed: 32109425]

Strichartz GR (1973). The inhibition of sodium currents in myelinated nerve by quaternary derivatives of lidocaine. The Journal of general physiology 62, 37–57. [PubMed: 4541340]

Stueber T, Eberhardt MJ, Hadamitzky C, Jangra A, Schenk S, Dick F, Stoetzer C, Kistner K, Reeh PW, Binshtok AM, et al. (2016). Quaternary Lidocaine Derivative QX-314 Activates and Permeates Human TRPV1 and TRPA1 to Produce Inhibition of Sodium Channels and Cytotoxicity. Anesthesiology 124, 1153–1165. [PubMed: 26859646]

Sterusky M, Plevkova J, Grendar M, and Buday T (2020). Female Guinea Pig Model for Cough Studies and Its Response to Most Common Tussive Substances. Physiol Res 69: S171–S179. [PubMed: 32228023]

Sun H, Kollarik M, and Undem BJ (2017). Blocking voltage-gated sodium channels as a strategy to suppress pathological cough. Pulm Pharmacol Ther 47, 38–41. [PubMed: 28522215]

Talbot S, Abdulnour RE, Burkett PR, Lee S, Cronin SJ, Pascal MA, Laedermann C, Foster SL, Tran JV, Lai N, et al. (2015). Silencing Nociceptor Neurons Reduces Allergic Airway Inflammation. Neuron 87, 341–354. [PubMed: 26119026]

Talbot S, Doyle B, Huang J, Wang JC, Ahmadi M, Roberson DP, Yekkirala A, Foster SL, Browne LE, Bean BP, et al. (2020). Vagal sensory neurons drive mucous cell metaplasia. The Journal of allergy and clinical immunology.

Tanaka M, and Maruyama K (2005). Mechanisms of Capsaicin- and Citric-Acid-Induced Cough Reflexes in Guinea Pigs. Journal of Pharmacological Sciences 99, 77–82. [PubMed: 16127241]

Udezue E (2001). Lidocaine inhalation for cough suppression. The American journal of emergency medicine 19, 206–207. [PubMed: 11326346]

Undem BJ, Carr MJ, and Kollarik M (2002). Physiology and plasticity of putative cough fibres in the Guinea pig. Pulm Pharmacol Ther 15, 193–198. [PubMed: 12099763]

Undem BJ, and Sun H (2020). Molecular/Ionic Basis of Vagal Bronchopulmonary C-Fiber Activation by Inflammatory Mediators. Physiology (Bethesda) 35, 57–68. [PubMed: 31799905]

Utsumi D, Matsumoto K, Tsukahara T, Amagase K, Tominaga M, and Kato S (2018). Transient receptor potential vanilloid 1 and transient receptor potential ankyrin 1 contribute to the progression of colonic inflammation in dextran sulfate sodium-induced colitis in mice: Links to calcitonin gene-related peptide and substance P. J Pharmacol Sci 136: 121–132. [PubMed: 29478714]

Watanabe N, Horie S, Spina D, Michael GJ, Page CP, and Priestley JV (2008). Immunohistochemical localization of transient receptor potential vanilloid subtype 1 in the trachea of ovalbumin-sensitized Guinea pigs. International archives of allergy and immunology 146 Suppl 1, 28–32. [PubMed: 18504403]

West PW, Canning BJ, Merlo-Pich E, Woodcock AA, and Smith JA (2015). Morphologic Characterization of Nerves in Whole-Mount Airway Biopsies. American journal of respiratory and critical care medicine 192, 30–39. [PubMed: 25906337]

Yamaki S, Chau A, Gonzales L, and McKemy DD (2021). Nociceptive afferent phenotyping reveals that transient receptor potential ankyrin 1 promotes cold pain through neurogenic inflammation

upstream of the neurotrophic factor receptor GFRα3 and the menthol receptor transient receptor potential melastatin 8. Pain 162: 609–618. [PubMed: 32826761]

Yeh JZ (1978). Sodium inactivation mechanism modulates QX-314 block of sodium channels in squid axons. Biophysical journal 24, 569–574. [PubMed: 728531]

Yin K, Deuis JR, Lewis RJ, and Vetter I (2016). Transcriptomic and behavioural characterisation of a mouse model of burn pain identify the cholecystokinin 2 receptor as an analgesic target. Mol Pain 12, 1744806916665366. [PubMed: 27573516]

Zaccone EJ, Lieu T, Muroi Y, Potenzieri C, Undem BE, Gao P, Han L, Canning BJ, and Undem BJ (2016). Parainfluenza 3-Induced Cough Hypersensitivity in the Guinea Pig Airways. PloS one 11, e0155526. [PubMed: 27213574]

Zhou C, Liang P, Liu J, Zhang W, Liao D, Chen Y, et al. (2014). Emulsified isoflurane enhances thermal transient receptor potential vanilloid-1 channel activation-mediated sensory/nociceptive blockade by QX-314. Anesthesiology 121: 280–289. [PubMed: 24667830]

Zielińska M, Jarmuż A, Wasilewski A, Sałaga M, and Fichna J (2015). Role of transient receptor potential channels in intestinal inflammation and visceral pain: novel targets in inflammatory bowel diseases. Inflamm Bowel Dis 21: 419–427. [PubMed: 25437822]

Bullet points:

What is already known

- Entry of the cationic lidocaine derivative QX-314 through activated TRP channels can silence nociceptive neurons.
- QX-314 co-applied with TRP channel activators can produce long-lasting inhibition of pain and itch.

What this study adds

- A more potent cationic compound, BW-031, can inhibit inflammatory pain without co-applied TRP activators.
- Inhaled BW-031 can also inhibit cough in guinea pigs.

Clinical significance

- Charged sodium channel blockers can be applied alone for long-lasting inhibition of inflammatory pain.
- Charged sodium channel blockers offer a novel mechanism for inhibiting cough associated with airway inflammation.

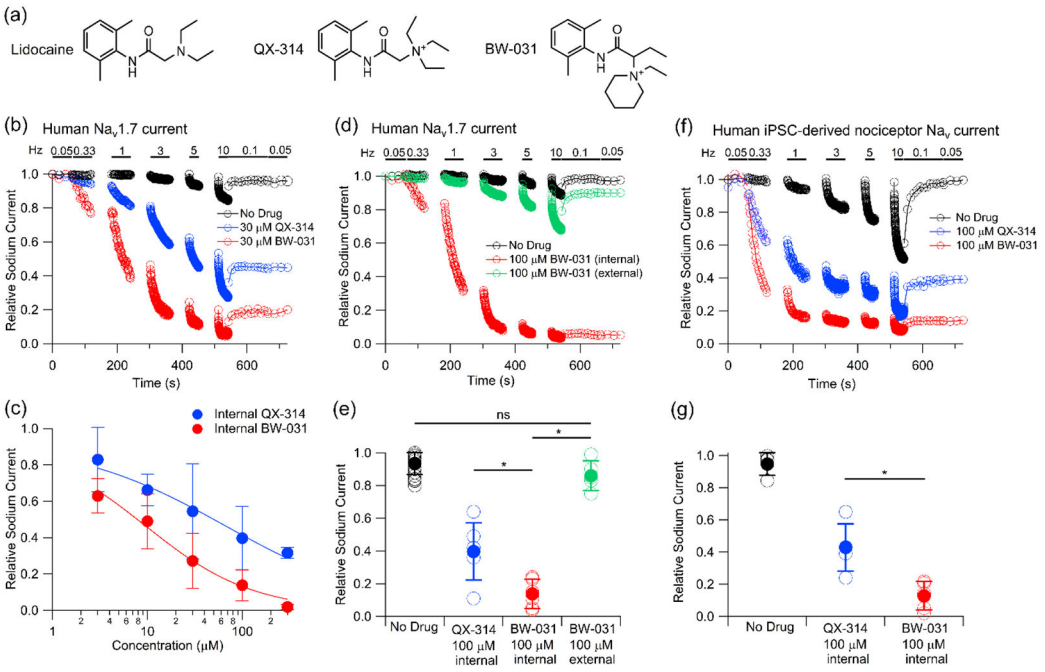

Figure 1. BW-031 inhibition of human Nav1.7 channels and sodium channels in iPSC-derived nociceptors.

(a) Chemical structures of lidocaine, QX-314 and BW-031. (b) Whole-cell patch clamp recordings illustrating use-dependent inhibition of $hNa_v1.7$ channels expressed in HEK 293 cells by 30 μM intracellular QX-314 (blue) or BW-031 (red) or with the use-dependent protocol run with control intracellular solution (black). $hNa_v1.7$ current was evoked by 20-ms depolarizations from −100 to −20 mV. After an initial stimulation at 0.05 Hz, trains of depolarizations at frequencies from 0.33 to 10 Hz were delivered, each for 1 minute (0.33 to 3 Hz) or 30 seconds (5 and 10 Hz), with a 1 minute rest between trains. (c) Dose-dependent inhibition by various intracellular concentrations of QX-314 (blue) and BW-031 (red). Mean±SD (n=6 for 3, 10, 30, 100, and 300 μM QX-314; n=6 for 3, 10, 30, and 100 μM BW-031, n=5 for 300 μM BW-031). Solid lines, best fits to (1/1 + [Drug]/IC_{50}), where [Drug] is the QX-314 or BW-031 concentration and IC_{50} is the half-blocking concentration, with IC_{50}=66 μM for QX-314 and IC_{50}=9.5 μM for BW-031. Current was quantified during the final slow (0.05 Hz) stimulation following the higher-frequency trains of stimulation. (d) Use-dependent inhibition of $hNa_v1.7$ channels (same voltage protocol as (a) by 100 μM intracellular BW-031 (red) contrasted with the same voltage protocol in control (black) or after application of 100 μM extracellular BW-031 (green). (e) Collected results for relative current remaining after the use-dependent pulse sequence for recordings of hNav1.7 currents with intracellular solution with no compound (black, n=37), intracellular 100 μM QX-314 (blue, n=6), intracellular 100 μM BW-031 (red, n=6), and extracellular 100 μM BW-031 (green, n=6). Asterisks indicate P<0.05. (f) Use-dependent inhibition (same protocol as in (a) and (d) of native Na_v currents in hiPSC-derived nociceptors by 100 μM intracellular QX-314 (blue) or 100 μM intracellular BW-031 (red), and Na_v currents in control neurons with compound-free intracellular solution with the same voltage protocol (black). (g) Collected results for relative current remaining after the use-dependent pulse sequence for recordings of Na_v currents in hiPSC-derived nociceptors with intracellular

solution containing no compound (black, n=4), intracellular 100 μM QX-314 (blue, n=5) and intracellular 100 μM BW-031 (red, n=5). Asterisks indicate $P<0.05$.

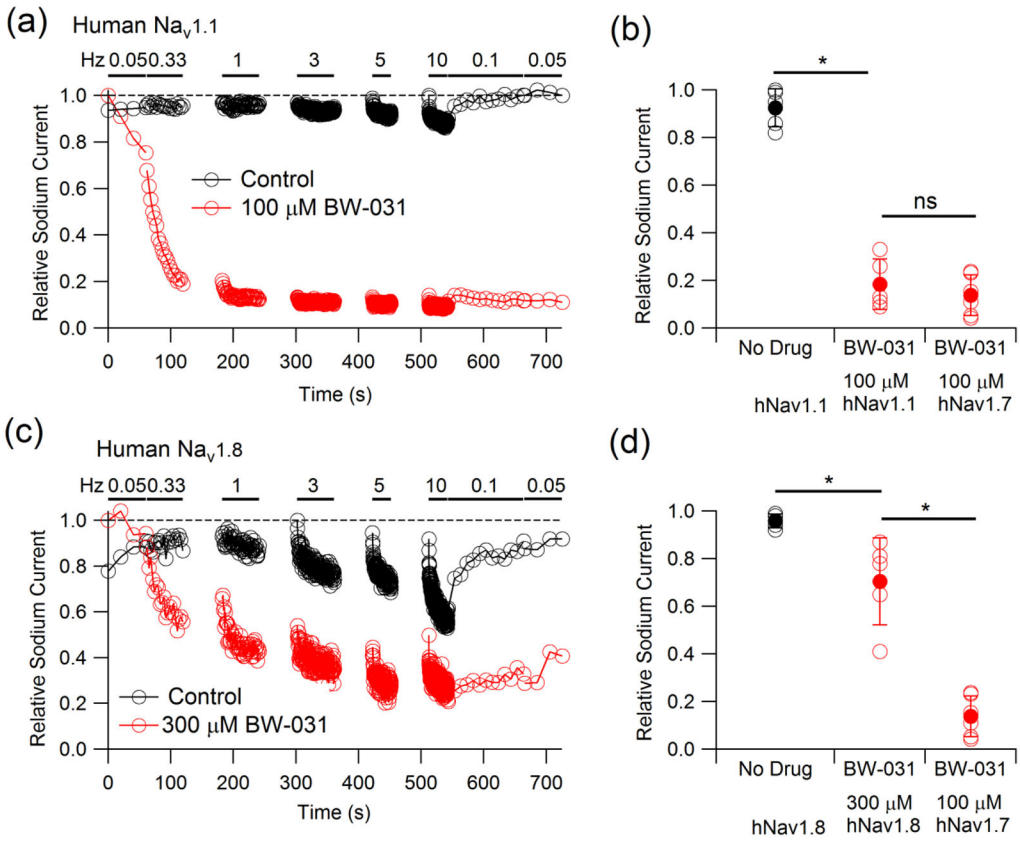

Figure 2. BW-031 inhibition of human Nav1.1 and Nav1.8 channels.

(a) Use-dependent inhibition of hNa$_v$1.1 channels by 100 μM intracellular BW-031 (red) compared to recording with control intracellular solution (black). Na$_v$ current was evoked by 20-ms depolarizations from −100 to 0 mV at the indicated frequencies. (b) Collected results for hNa$_v$1.1 inhibition by 100 μM intracellular BW-031 (red, n=5) compared with control (black, n=5) and with inhibition of hNa$_v$1.7 (n=6, replotted from Figure 1e). (c) Use-dependent inhibition of hNa$_v$1.8 channels by 300 μM intracellular BW-031 (red) compared to recording with control intracellular solution (black). Na$_v$ current was evoked by 20-ms depolarizations from −70 to 0 mV at the indicated frequencies. (d) Collected results (mean±SD) of hNa$_v$1.8 inhibition by 300 μM intracellular BW-031 (red, n=5) compared with control (black, n=5) and with inhibition of hNa$_v$1.7 by 100 μM BW-031 (n=6, replotted from Figure 1e). Asterisks indicate P<0.05.

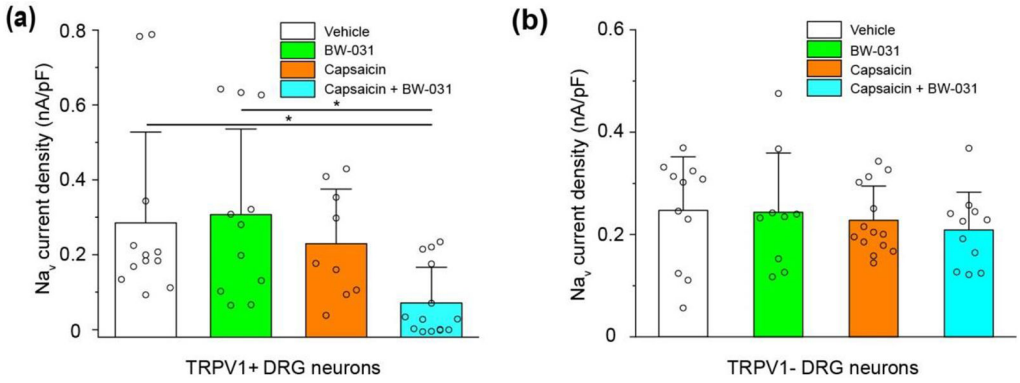

Figure 3. Extracellular application of BW-031 to DRG neurons inhibits sodium currents only with concomitant activation of TRPV1 channels.

(a) Quantification of voltage-clamp recordings of sodium currents in TRPV1+ mouse DRG neurons pre-treated with vehicle (white), 100 μM BW-031 (green), 1 μM capsaicin (orange) or 1 μM capsaicin + 100 μM BW-031 (cyan). Capsaicin facilitates the inhibition of Na_v currents in mouse TRPV1+ DRG neurons treated with BW-031. N=12 cells for vehicle, n=11 for BW-031 alone, n=9 for capsaicin alone, n=14 for capsaicin + BW-031. (b) Quantification of the Na_v current density data from TRPV1− DRG neurons pre-treated with vehicle (white), 100 μM BW-031 (green), 1 μM capsaicin (orange) or 1 μM capsaicin + 100 μM BW-031 (cyan). Capsaicin does not facilitate the block of Na_v channels in mouse TRPV1− DRG neurons treated with BW-031. N=11 cells for vehicle, n=9 for BW-031 alone, n=13 for capsaicin alone, n=10 for capsaicin+BW-031. Individual data points are displayed as open circles. Bars represent mean±SD for each condition. Asterisks indicate $P<0.05$.

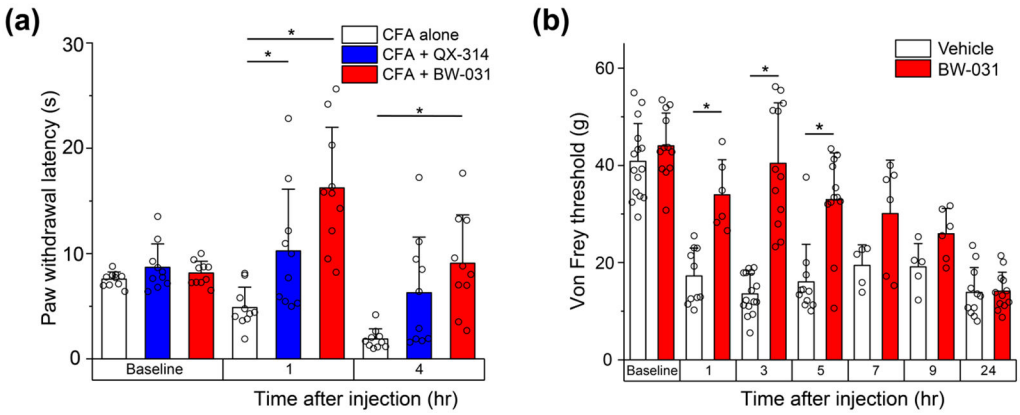

Figure 4. BW-031 produces long-lasting analgesia in rat paw CFA injection and surgical paw incision pain models.

(a) Hargreaves assay of hindpaw thermal sensitivity in rats after intraplantar injection of Complete Freund's Adjuvant (CFA) alone (white), 2% QX-314 dissolved in CFA (blue) or 2% BW-031 dissolved in CFA (red). Both QX-314 and BW-031 produce robust thermal analgesia. N=10 male rats per group. (b) Von Frey measurements of hindpaw mechanical sensitivity in male rats after paw incision and intraplantar injection of vehicle or 2% BW-031. Baseline measurements were made before paw incision. Vehicle or 2% BW-031 was injected 24 hours after the incision. For vehicle group: n=15 for baseline, n=10 for 1 hr, n=15 for 3 hrs, n=11 for 5 hrs, n=5 for 7 hrs, n=5 for 9 hrs, n=11 for 24 hrs. For BW-031-treated group: n=12 for baseline, n=6 for 1 hr, n=12 for 3 hrs, n=12 for 5 hrs, n=6 for 7 hrs, n=6 for 9 hrs, n=12 for 24 hrs. Because of the time required for each measurement, not all animals in each group could be assayed for every time point. Animals were chosen at random for times at which not all could be assayed. Individual data points are displayed as open circles. Bars represent mean±SD for each condition. Asterisks indicate $P<0.05$.

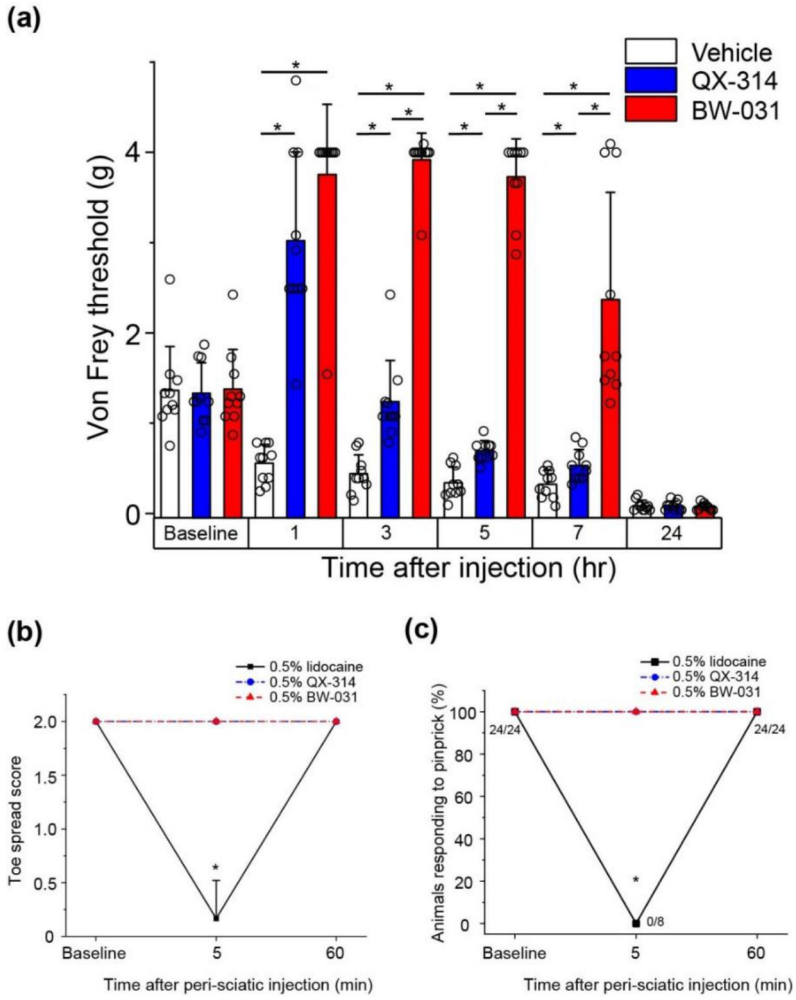

Figure 5. BW-031 produces long-lasting analgesia in a mouse paw UV-burn model and has no effect on sensory or motor function with perisciatic injection in naïve mice.

(a) Von Frey measurements of hindpaw mechanical sensitivity in male mice after plantar UV-burn and intraplantar injection of vehicle, 2% QX-314 or 2% BW-031. N=10 mice per group. Bars represent mean±SD for each condition. Asterisks indicate P<0.05.

(b) Toe spread assay of motor function in naïve male mice after perisciatic injection of 0.5% lidocaine, 0.5% QX-314 or 0.5% BW-031. Lidocaine produces robust block of motor function in naïve mice at 5 min with recovery at 60 min. QX-314 had no effect. N=10 mice per group. Data are mean±SD. Asterisk indicates P<0.05. (c) Plantar pinprick responses in naïve male mice after perisciatic injection of 0.5% lidocaine, 0.5% QX-314 or 0.5% BW-031. Lidocaine produces robust block of pinprick response in naïve mice at 5 min with recovery at 60 min. Neither QX-314 nor BW-031 had any effect. N=8 mice per group. Data are mean±SD. Asterisks indicate P<0.05.

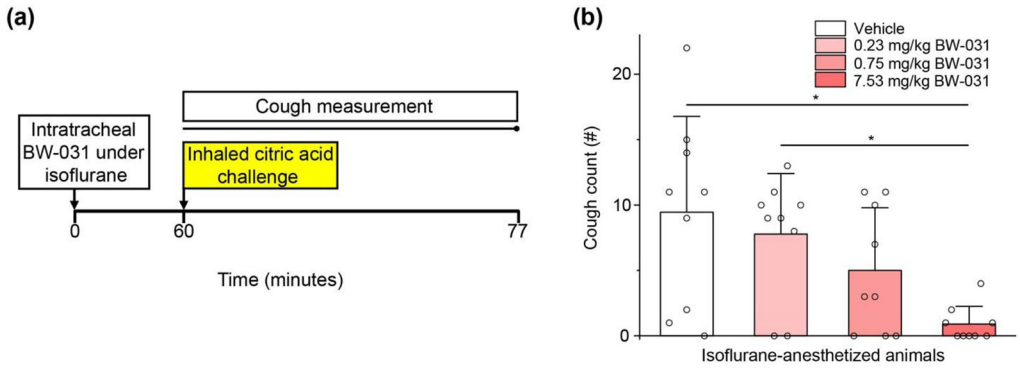

Figure 6. Intratracheal delivery of BW-031 under isoflurane anesthesia inhibits citric acid-evoked cough in guinea pigs.

(a) Experimental design. BW-031 (0.23, 0.75 or 7.53 mg/kg) was delivered intratracheally to guinea pigs under isoflurane anesthesia. One hour later, the animals inhaled an aerosol with 400 mM citric acid for 7 minutes (yellow) and coughs were measured over 17 minutes during and after the citric acid challenge. (b) Dose-dependent effect of intratracheal BW-031 on citric acid-evoked cough. N=9 female guinea pigs per group. Individual data points are displayed as open circles. Bars represent mean±SD for each condition. Asterisks indicate $P<0.05$.

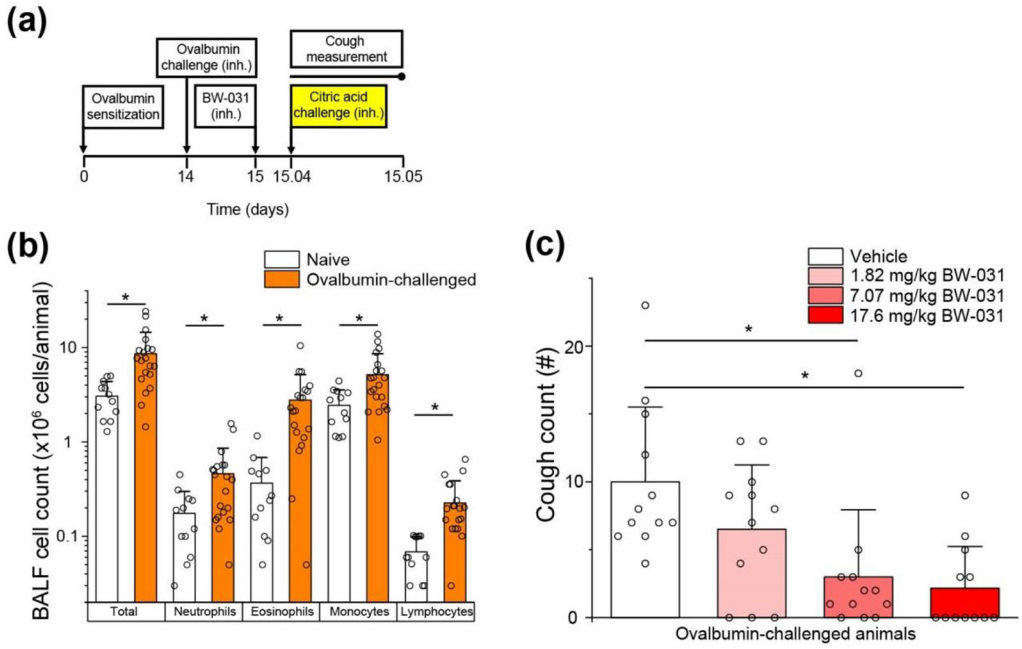

Figure 7. BW-031 inhibits cough in guinea pigs following allergic airway inflammation.

(a) Experimental design. Guinea pigs were sensitized with intraperitoneal and subcutaneous ovalbumin and challenged with inhaled (inh.) ovalbumin two weeks later. One day after ovalbumin challenge, the animals inhaled BW-031 (inhaled doses of 1.82, 7.07 or 17.6 mg/kg BW-031) followed one hour later by inhalation of 400 mM citric acid (yellow) for 7 minutes. Cough counts were measured for 17 minutes during and following the citric acid challenge. (b) Ovalbumin sensitization and challenge causes lung inflammation, as measured by immune cell counts in bronchoalveolar lavage (BAL). N=20 animals for naïve group (1:1 male:female), N=12 animals for ovalbumin-sensitization group (1:1 male:female). Individual data points are displayed as open circles. Bars represent mean±SD for each condition. Asterisks indicate $P<0.05$.

(c) Inhaled BW-031 produces dose-dependent inhibition of citric acid-evoked cough following allergic airway inflammation. N=12 animals per group (1:1 male:female). Individual data points are displayed as open circles. Bars represent mean±SD for each condition. Asterisks indicate $P<0.05$.

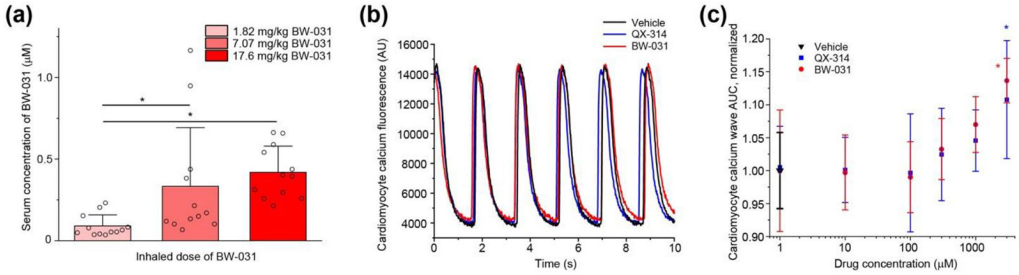

Figure 8. Inhaled BW-031 has minimal systemic distribution and is not cardiotoxic.

(a) Serum concentrations of BW-031 following inhalation. N=12 animals per group (1:1 male:female). Individual data points are displayed as open circles. Individual data points are displayed as open circles. Bars represent mean±SD for each condition. Asterisks indicate $P<0.05$. (b) Representative calcium fluorescence signals from hiPSC-derived cardiomyocytes treated with vehicle, 100 μM QX-314 or 100 μM BW-031. (c) Quantification of the effect of QX-314 and BW-031 on cardiomyocyte calcium signals as measured by area under the curve (AUC). Micromolar doses of QX-314 or BW-031 do not affect cardiomyocyte calcium signal AUC. N=10 wells for vehicle, n=5 wells for each concentration of QX-314. Bars represent mean±SD for each condition. Asterisk indicates $P<0.05$.